Bralower, T.J., Premoli Silva, I., and Malone, M.J. (Eds.)
Proceedings of the Ocean Drilling Program, Scientific Results Volume 198

17. A Petrological and Geochemical Study of Cretaceous Siliceous Rocks from Shatsky Rise[1]

Kristin Fontilea,[2] Kathleen M. Marsaglia,[2] and Norman Dean[3]

ABSTRACT

Samples of chert, porcellanite, and chalk/limestone from Cretaceous chert-bearing sections recovered during Leg 198 were studied to elucidate the nature and origin of chert color zonations with depth/age. Sedimentary structures, trace fossils, compactional features, sediment composition, texture, geochemistry, and diagenetic history were compared among lithologies. Trends in major and minor element composition were determined. Whereas geochemical analyses demonstrate systematic elemental differences among the different lithologies, there are less distinct patterns in composition for the colored cherts. The color of the chert appears to be related primarily to the amount of silica and secondarily to the proportion of other components. Red cherts are almost pure silica with only minor impurities. This may allow pigmentation from fine Fe oxides to dominate the color. These red cherts are from places where geophysical logs indicate that chert is the dominant rock type of the section. These red chert intervals cannot be unequivocally distinguished from surrounding chert-bearing lithologies in terms of sedimentary structures.

INTRODUCTION

During previous Deep Sea Drilling Project (DSDP) and Ocean Drilling Program (ODP) legs on Shatsky Rise, recovery of Cretaceous units was hampered by the presence of chert intervals (Bralower, Premoli Silva, Malone, et al., 2002). One objective of ODP Leg 198 was to more suc-

[1] Fontilea, K., Marsaglia, K.M., and Dean, N., 2006. A petrological and geochemical study of Cretaceous siliceous rocks from Shatsky Rise. *In* Bralower, T.J., Premoli Silva, I., and Malone, M.J. (Eds.), *Proc. ODP, Sci. Results,* 198, 1–45 [Online]. Available from World Wide Web: <http://www-odp.tamu.edu/publications/198_SR/VOLUME/CHAPTERS/107.PDF>. [Cited YYYY-MM-DD]
[2] Department of Geological Sciences, California State University Northridge, 18111 Nordhoff Street, Northridge CA 91330-8266. Correspondence author: **kristinfontilea@mac.com**
[3] Department of Chemistry and Biochemistry, California State University Northridge, 18111 Nordhoff Street, Northridge CA 91330-8266.

Initial receipt: 1 March 2004
Acceptance: 14 September 2005
Web publication: 27 March 2006
Ms 198SR-107

cessfully recover chert-bearing horizons using new drilling techniques such as the motor-driven core barrel. Despite these attempts, full recovery of these intervals remained elusive during Leg 198. However, short, relatively intact sections of chert and associated porcellanite and unaltered chalk were recovered throughout the Shatsky Cretaceous section (Berriasian to Maastrichtian) at Site 1207 on the Northern High and at Sites 1213 and 1214 on the Southern High (Fig. F1). Chert in the Cretaceous sections is highly variegated, with colors of pink, orange, red, brown, yellow, olive, gray, and black (Figs. F2, F3, F4). Cyclic changes in chert color across the Cretaceous interval were linked by shipboard scientists to changes in rates of sediment accumulation (Bralower, Premoli Silva, Malone, et al., 2002). Furthermore, some of these intervals were successfully logged, providing new information on the character and distribution of the chert intervals. This project is a petrological and geochemical study of these Cretaceous cherts and associated sedimentary rocks (porcellanite/chalk), focusing on chert color and its implications for depositional and diagenetic history. In particular, we document the nature (composition, mineralogy, and texture) of chert, porcellanite, and chalk/limestone at Site 1213. Note that the Aptian section containing the Selli oceanic anoxic event (OAE1a) is discussed elsewhere (Marsaglia, this volume).

TERMINOLOGY OF SILICEOUS ROCKS

Chert and porcellanite are field terms used by shipboard scientists to differentiate fine-grained siliceous sedimentary rocks based on their textural and physical properties (Hesse, 1990). Porcellanite is the term used to describe a porous siliceous sedimentary rock with a dull or matte luster similar to unglazed porcelain, whereas chert is the term used to describe a dense, vitreous, hard, and brittle rock (Bramlette, 1946). Pisciotto (1980) defines chert similarly as a hard, conchoidally fracturing, cryptocrystalline, varicolored sedimentary rock with semivitreous, vitreous, or waxy luster, consisting dominantly of silica. He describes porcellanite as a siliceous sedimentary rock with a dull or matte luster resembling that of unglazed porcelain that is less hard, dense, and vitreous than chert and commonly has lower silica content.

Siliceous rocks have also been categorized by mineralogical composition. Isaacs (1981a) classifies siliceous rocks mainly on the relative abundance of silica and detrital minerals; silica ranges from 20% to 90%, and the ratio of silica to detrital minerals ranges from 0.3 to 9.0. Where silica is diagenetic, physical properties are closely related to the silica/detrital ratio. This ratio is >3.0 (~75% silica) in cherts and cherty porcellanites, 1.25–5.0 (~22%–55% silica) in porcellanites, and <1.0 (~50% silica) in siliceous shales and siliceous mudstones. Opal A is transformed to quartz at increasing temperatures, decreasing the silica to detrital mineral ratio, and opal-CT subsequently transforms to quartz at increasingly lower temperatures (Isaacs, 1981b). Jones and Murchey (1986) also use detrital clay mineral content to differentiate between chert and porcellanite. The higher (25%–50%) clay mineral content corresponds to porcellanite, whereas the lower clay content (0%–25%) corresponds to chert.

Cherts of deepwater origin can also be bedded or nodular, with nodular structures ascribed solely to diagenetic processes and bedded units ascribed to variations in surface water productivity or terrigeneous sediment input, overprinted by diagenesis (Hesse, 1990).

F1. Location map, p. 13.

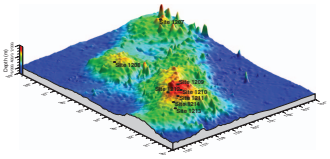

F2. Colors of chert recovered from Hole 1207B, p. 14.

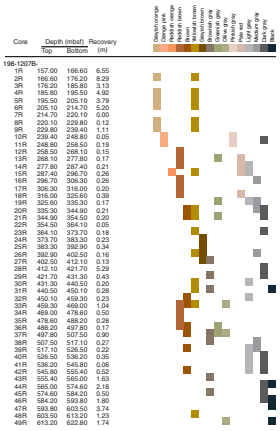

F3. Colors of chert recovered from Site 1213, p. 15.

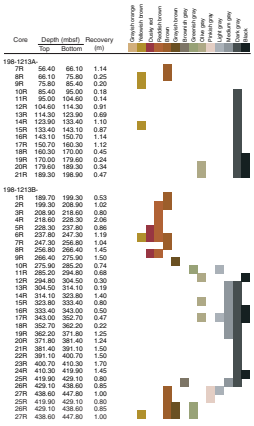

F4. Colors of chert recovered from Hole 1214A, p. 16.

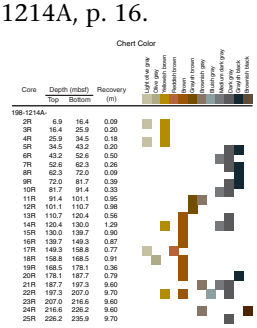

BACKGROUND

Few studies have examined the nature of chert color variation, particularly in deep-sea cores. Luedtke (1978), Fraser et al. (1972), and Hein et al. (1981) reported geochemical analyses of siliceous rocks (Table T1), but they did not focus specifically on the elemental differences among the different colors of chert. Hein et al.'s (1981) study is perhaps the most relevant to our discussion in that they analyzed some Cretaceous chert samples from Pacific sections (Table T1). They found that higher carbonate content in the chert samples correlated with high values of Mg, Ca, Mn, Sr, and Zr, whereas tuffaceous cherts were characterized by high values of K, Al, Zn, Mo, and Cr. Purer cherts had high SiO_2 and boron values. No studies of Cretaceous chert-bearing sections have described alternating stratigraphic changes in color similar to those documented by Bralower, Premoli Silva, Malone, et al. (2002) on Shatsky Rise. However, Douzen and Ishiga (1995) reported stratigraphic changes in chert color from reddish to gray in Triassic and Jurassic outcrops of deep-marine sections near Japan and suggested that these represent changes in bottom conditions from oxic to anoxic.

T1. Chert color and trace element composition, p. 32.

Although trends in chert color with age and sedimentation rate have been documented at Sites 1207, 1213, and 1214 (Figs. F2, F3, F4) (Bralower, Premoli Silva, Malone et al., 2002), the combination of samples from Sites 1207 and 1213 provides the most complete temporal coverage of the Cretaceous chert-bearing intervals and represents the paleolatitudinal range from north (Site 1207) to south (Site 1213) across Shatsky Rise. We focus first on Site 1213, which has the most pronounced color variations over the longest stratigraphic record (Cenomanian to Berriasian). Shipboard analysis of color patterns within the Cretaceous chert-bearing intervals showed a distinct correlation between color and sedimentation rate throughout the section at Site 1213. Rough color zonations at Site 1213 (Fig. F3) are as follows:

56–85 meters below seafloor (mbsf) = red/brown,
85–189 mbsf = gray/black,
189–266 mbsf = red/brown,
266–400 mbsf = gray/black, and
400–447 mbsf = red/brown.

The sedimentation rates range from 12 to 21 m/m.y. in the gray/black zones and from 1 to 5 m/m.y. in the red/brown zones (Bralower, Premoli Silva, Malone, et al., 2002). Thus, it follows that the colors likely reflect sedimentation rates, with the reddish hues being associated with slower sedimentation and more oxidizing conditions.

In contrast, chert-bearing intervals at Site 1207 range from Campanian to Barremian in age, with only a minor gap at the Turonian/Coniacian boundary. There are less distinct color trends at Site 1207 and a tendency for the presence of both red/brown and gray/black chert in many cores. The indistinct color changes at Site 1207 may be a product of downhole contamination coupled with the overall lower sedimentation rates. Furthermore, as this was the first chert section described during Leg 198, some of the variation may be due to inconsistencies in description techniques.

METHODS

Cores from Site 1207 were reexamined and described (Fig. F5) at the ODP Gulf Coast Core Repository at Texas A&M University (USA) in order to verify color trends from original shipboard descriptions (Fig. F2). It is not known if the original shipboard descriptions were based on wet vs. dry chert or whether all visible chert colors or only the predominant chert colors were recorded. Chert was wetted prior to description, and color was classified using a Geological Society of America (GSA) rock color chart (Rock-Color Chart Committee, 1991). Sampling was limited to the base of the section (Barremian) at this site (Fig. F6), an interval not cored at Sites 1213 and 1214.

A total of 95 sample chips were collected from core recovered during Leg 198, mainly from Site 1213, but additional samples were collected from Sites 1207 and 1214 (Table T2). Sample intervals were chosen where stratigraphy was most intact, as well as where a variety of lithologies were present. Whenever possible, at least one sample of chalk, porcellanite, and chert was taken per core, and if different colors of chert were present, each major color was sampled. All sample chips were described in terms of color, composition, and sedimentary structures using a hand lens, stereoscopic microscope, and GSA color chart.

Once described, 55 of the 95 chosen samples of chert, porcellanite, and chalk/limestone were selected for thin section preparation (Fig. F6; Table T3). These samples were split (cut), and a subsample was impregnated with blue-dyed epoxy, which highlights microporosity distribution, prior to thin section production. The 55 thin sections were described using a petrographic microscope for composition, mineralogy, texture, lithology, and chert color, as well as visual estimations of percentages of components (Table T3).

Hand-specimen and thin-section descriptions were used to select representative samples of chert, porcellanite, and chalk/limestone for geochemical analyses using X-ray fluorescence (XRF) at Washington State University GeoAnalytical Laboratory (USA). Sample selection was based on volume, uniformity of lithology, availability of other nearby lithologies for comparison, age of units, and chert color. A total of 28 samples were chosen from Site 1213, and two were chosen from the base of Site 1207 (Fig. F6; Table T3). This set of samples includes 20 cherts (four red, nine brown, six gray, and one green), two porcellanitic cherts, one porcellanite, one siliceous limestone, and five limestones (lithologies based on X-ray diffraction [XRD] data). Samples were analyzed for major and trace elements, including Si, Al, Ti, Fe, Mn, Ca, Mg, K, Na, P, Ni, Cr, Sc, V, Ba, Rb, Sr, Zr, Y, Nb, Ga, Cu, Zn, Pb, La, Ce, and Th (Table T4). This is done by measuring and comparing the X-ray intensity for each element with the intensity for two beads each of nine US Geological Survey standard samples and two beads of pure vein quartz (used as blanks for all elements except Si). The 20 standard beads are run and used for recalibration approximately once every 3 weeks or after the analysis of ~300 unknowns. Intensities for all elements are corrected automatically for line interference and absorption effects. For each element, the limit of determination, the 2-σ uncertainty in precision, is reported (Table T4). Normalized data for each element, major and trace, was analyzed to determine similarity among varying rock types and colors. Loss on ignition (LOI), SO_3, and Cl values (found using QuantAs semiquantitative scans) were also determined for most samples. SO_3 and Cl were present in small to moderate amounts in

F5. Colors of chert recovered from Hole 1207B, p. 17.

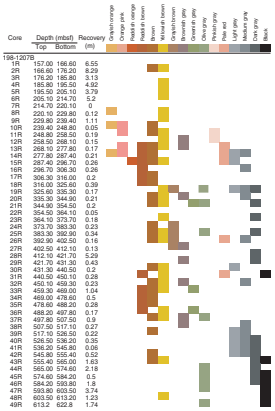

F6. Lithostratigraphy at Sites 1207, 1213, and 1214, p. 18.

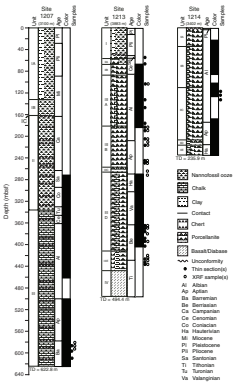

T2. Hand specimen descriptions, p. 33.

T3. Petrographic observations and visual estimates, p. 38.

T4. XRF data, p. 40.

some samples. Iron (II) vs. iron (III) was not differentiated, as the XRF technique can only detect iron atoms, not the valence state. No other elements, with the exception of W and Co (which are present at a few hundred ppm because of grinding bowl contamination), were detected.

Several of the samples total <98 wt% and, according to the criteria of Ragland (1989) for igneous rocks, are not acceptable. They are generally samples with high CaO contents and correspondingly high LOI values, essentially limestones and calcareous lithologies as verified by thin section and XRD analyses. The low weight percent totals could be due to several factors, including the presence of elements not analyzed. LOI was determined at 750°C, a temperature that might not have completely calcined carbonate minerals present. Some of the missing weight percent could also be associated with sulfur. Note that no distinct barite or gypsum/anhydrite peaks were noted in the XRD patterns (see below), but minor pyrite is present. The data were normalized (scaled proportionately) to 100% in order to compensate for these unanalyzed elements (e.g., C and S); this allows for sample comparison.

Powder diffraction data were collected on an Oxford Diffraction Xcalibur3 diffractometer equipped with a molybdenum X-ray source (2.0 kW; 1.00-mm beam diameter) and a Saphire3 charge-coupled device detector. Samples powdered using a small microdrill were packed into X-ray quality 0.70 mm glass capillary tubes that were then sealed and affixed to a brass pin. The samples were mounted on a Huber goniometer head and aligned in the X-ray beam. The data collection procedure was as follows: with the detector set 50 mm from the sample, a 5-min measurement of the CCD dark current was performed followed by two 5-min data collections over a 360° ϕ rotation of the sample. The two images were compared to remove any anomalous signals and then integrated and converted to a two-dimensional powder pattern using the Crysalis software package (**www.oxford-diffraction.com**). The data were exported to Microsoft Excel for analysis. A blank scan was obtained by mounting an empty capillary tube and collecting a data set using identical conditions. Baseline corrections on the samples were performed by a simple point by point subtraction of a scaled value of the blank measurement. The scale factor was chosen to provide as flat a baseline as possible while maintaining an overall positive intensity measurement in the corrected data set. Peak values were compared to known mineral diffraction data (e.g., silica minerals [α-quartz, cristobalite, and tridymite], carbonate minerals, etc.).

RESULTS

Verification of Color Trends at Site 1207

Discrete downhole trends in color were documented at Sites 1213 and 1214, but a more mixed pattern was observed at Site 1207 (Fig. **F2**), which we questioned. Results of the reexamination and description of Site 1207 cores are given in Figure **F5;** these proved similar to the original shipboard descriptions with some minor variations in color (Fig. **F2**), verifying the mixed pattern. In general, Site 1207 (Figs. **F2, F5**) shows a general color trend of predominantly yellowish brown chert in Cores 198-1207B-1R through 10R, whereas Cores 198-1207B-10R through 32R display a wide range of chert colors, including grays. The gray cherts do not occur in Cores 33R through 37R, and then reappear in Core 38R.

Another question about the color patterns at Site 1207 concerned the wide variety of chert colors, from brown to black hues, observed in individual cores (Figs. F2, F5). Chert fragments were reexamined to determine if there is in fact a tendency for chert to be more variegated at Site 1207. Out of the 184 fragments described to create Figure F5, only 13% (24) were variegated; the remaining fragments exhibited only one color.

Petrographic Descriptions

In general, the lithologies, mineralogies, structures, and textures of samples (Tables T2, T3) are similar to those described at Site 1207 (Bralower, Premoli Silva, Malone et al., 2002) and by previous workers for Cretaceous sedimentary rocks from Shatsky Rise (Keene, 1975) and other Pacific sites (Hein et al., 1981). As our focus is chert color, we looked for attributes associated with color and found grossly defined trends. In terms of biogenic components, radiolarian percentages were highest in the brown chert, intermediate in the gray chert, and lowest in the red chert. Foraminifer percentages decreased from reddish brown to brown to dark gray chert, whereas ostracodes were most common in the reddish brown cherts. Lamination and bioturbation also showed patterns, particularly in the gray lithologies. Distinct burrows were more common in the dark gray chert, porcellanite, and limestone; lamination was most common in the gray limestone. Diagenetic features were also analyzed; the only trend was that reddish brown chert showed the highest percentage of opal-CT lepispheres filling bioclasts. There was no trend in porosity type or abundance with color, which is more of a function of lithology, with the chalk/limestones having the highest percentage of matrix porosity and the cherts having the lowest.

Organic matter content was petrographically estimated (Table T3), and values ranged up to ~2%. Organic content in red chert samples was not distinguishable, owing to the presence of Fe oxides. Two brown cherts had moderate (~2%) organic matter content, whereas seven brown and three gray chert samples had low (~1%) organic matter content. Of the remaining chert samples, 11 brown, 15 gray, and 1 green had negligible (<1%) amounts of organic matter.

Geochemical and X-Ray Diffraction Data

Geochemical data are presented in Table T4 and Figures F7, F8, F9, F10, F11, F12, F13, F14, F15, F16, and F17. In some samples elements generally considered as trace elements occur in sufficient quantities to be considered major elements (e.g., Ba and Sr) (Table T4) but are still discussed below with the trace components. A coefficient correlation analysis of XRF data was performed in order to determine significant positive (>0.80) or negative (less than –0.80) correlations among major elements and trace elements within the sample set (Table T5). Significant positive correlation exists among the following groups: TiO_2, Al_2O_3, MgO, Na_2O, K_2O, Rb, Sr, Zr, and Zn; FeO, MgO and Cu; P_2O_5 and La; and V and Ba. A negative correlation exists between SiO_2 and TiO_2, Al_2O_3, MgO, CaO, Sr, Zr, and Zn.

Major Element Analyses

As expected in a suite of chert, porcellanite, and chalk/limestone samples, the major elemental components are silica (SiO_2), mainly representing opal (-A and -CT), chalcedony, and microquartz, and calcium

F7. Normalized percentages of SiO_2 and CaO, p. 19.

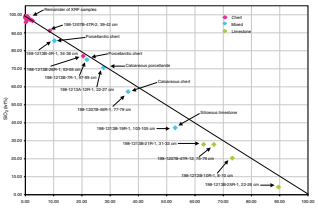

F8. Concentration of barium, p. 20.

F9. Concentration of strontium, p. 21.

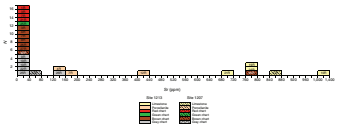

F10. Concentration of titanium, p. 22.

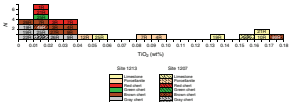

F11. Concentration of aluminum, p. 23.

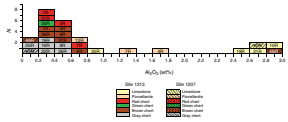

F12. Concentration of magnesium, p. 24.

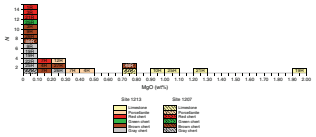

F13. Concentration of potassium, p. 25.

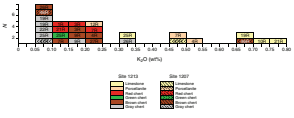

(CaO), representing biogenic and authigenic carbonate components. Low aluminum content indicates only trace amounts of clay minerals (or feldspar) in these pelagic rocks. XRF data indicate some end-member lithologies, but many samples are mixtures of silica and carbonate phases. Sample mineralogy was verified using XRD techniques. The XRF and XRD data were used to reclassify the samples (Table T6). Three of the samples showed evidence of common to abundant cristobalite, confirming that the samples are porcellanite or porcellanitic chert. Four samples contain abundant calcite, confirming that they are limestones. Two are mixed limestone/chert. The remainder are chert.

To illustrate the above relationships, the weight percent SiO_2 and CaO contents of the samples are plotted by lithology in Figure F7. All samples that significantly deviate from the 1:1 ratio line (e.g., Cores 198-1213B-25R, 10R, 198-1207B-47R, 198-1213B-21R, 19R, and 198-1207B-46R) contain high concentrations of barium (3,104–12,361 ppm) (Fig. F8). The samples with the greatest deviation (Cores 198-1213B-10R and 109-1207B-46R) tend to show higher concentrations of strontium (764–1026 ppm) (Fig. F9) and aluminum oxide (~3 wt%).

Major element distributions (Figs. F10, F11, F12, F13, F14, F15, F16, F17) show some trends among percent composition vs. lithology. Titanium percentages are generally low (0.18–0.006 wt%), aluminum content ranges up to 2.9 wt%, magnesium ranges up to 1.92 wt%, sodium ranges up to 0.69 wt%, and potassium ranges up to 0.80 wt%. These five components (Ti, Al, Mg, Na, and K) are most common in limestones and porcellanite and less abundant in chert. Limestones contain the most iron, but a few chert samples are also ferruginous. Iron percentages range up to 3.5 wt%. Manganese and phosphorous do not vary systematically with lithology. Manganese content ranges up to 1.6 wt%, whereas phosphorus ranges up to 0.49 wt%.

There are a few trends relating major element composition to chert color. With a few exceptions, gray cherts generally have lower concentrations of Fe and K than red and brown cherts. Brown cherts contain higher Mn or P and variable though moderate concentrations of trace elements. Gray cherts have lower Al and higher Ca. Chert color vs. aluminum content appears to be somewhat variable, but in general, gray cherts have the least amount of aluminum. Chert color shows no systematic relationship with magnesium, sodium, or titanium contents.

Minor Element Analyses

Several trace elements, such as Ni, Cr, La, Ce, and Ga, show no systematic relationship to lithology and major element percent composition (Table T4). Most trace elements, such as Sc, Rb, V, Zr, Nb, Zn, Y, Cu, Sr, and Ba, generally are most abundant in limestones and porcellanites, but show no apparent trend with chert color (Table T4; Figs. F8, F9).

Chert/Porcellanite/Limestone Suites

XRF data (Table T4) were also analyzed to determine whether there were any correlations between major and trace element composition of chert and closely associated (same core) porcellanite or limestone. The samples selected for XRF analyses included six sets of chert and associated porcellanite or limestone from the same core segment or from the same core interval. These pairs include

1. Limestone and gray chert from Core 198-1213B-19R;

F14. Concentration of iron, p. 26.

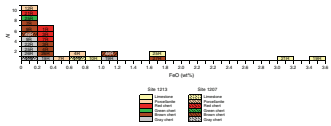

F15. Concentration of manganese, p. 27.

F16. Concentration of phosphorus, p. 28.

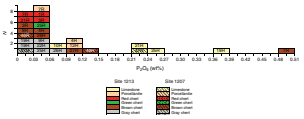

F17. Concentration of sodium, p. 29.

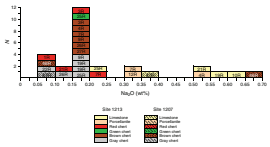

T5. Coefficient correlation matrix, p. 44.

T6. XRD data, p. 45.

2. Limestone and green chert from Core 198-1213B-25R;
3. Limestone (reclassified as calcareous chert based on XRF/XRD) and brown chert from Core 198-1207B-46R;
4. Porcellanite (reclassified as porcellanitic chert based on XRF/XRD) and brown chert from Core 198-1213B-4R;
5. Porcellanite (reclassified as porcellanitic chert, based on XRF/XRD) and red chert from Core 198-1213B-7R; and
6. Porcellanite and gray chert from Core 198-1207B-47R.

With respect to major element compositions, several gross trends are apparent. The greatest difference in Fe content is seen between gray chert and its associated limestone, although both lithologies are generally enriched in Fe compared to other non-gray lithology counterparts. The gap between chert vs. limestone Fe content narrows in the green and brown chert-limestone pairs, and is even narrower between chert and porcellanite. Magnesium shows the same trend as iron. Other significant observations may have bearing on chert color. The limestone associated with the green chert has very high Mn, and the chert is also slightly enriched in Mn compared to other chert colors. The porcellanite (porcellanitic chert) associated with brown and red cherts has slightly less Mn than its chert counterpart. In addition to the red chert porcellanite pair in Core 198-1213B-7R, another red chert sample was analyzed. Notably, the brown chert has much higher P content.

Similarities in trace element composition were observed in three of the sample pairs. Limestone and green chert from Core 198-1213B-25R have similar contents of Cr (both 11 ppm), Sc (0 and 1 ppm, respectively), and Rb (9 and 8 ppm, respectively). The porcellanite (porcellanitic chert) and red chert from Core 198-1213B-7R have similar Ce contents of 13 and 10 ppm, respectively. The porcellanite and gray chert from Core 198-1207B-47R have similar Ni contents of 9 and 8 ppm, respectively. Aside from these trends, no other commonalities were observed.

Geophysical and Geochemical Logs

Interpretations by shipboard scientists of downhole geophysical and geochemical logs at Sites 1207 and 1213 provide some additional information for understanding the stratigraphic distribution of chert in the section. This is especially important given the low recovery rates in the Cretaceous chert-bearing sections, so we attempt to correlate chert color distribution to these data.

The Formation MicroScanner (FMS) provides high-resolution electrical resistivity–based images of borehole walls, which allowed shipboard scientists to determine chert distribution, thickness, and percentage over the interval from 200 to 380 mbsf in Hole 1207B (Bralower, Premoli Silva, Malone et al., 2002). FMS data indicate that the chert is layered (continuous across borehole), not nodular (curved edge exposed in borehole), and that chert bed thickness ranges from 0.025 to 0.25 m (Fig. F18) (Bralower, Premoli Silva, Malone, et al., 2002). Note that the descriptive term layered is used rather than the term bedded, which has implications for the origin of the chert. Our addition of the chert color trends on Figure F18 shows that the thickest chert intervals occur within the uppermost yellow to yellow-brown chert sequence from 200 to 278 mbsf. The interval from 306 to 326 mbsf shows the highest percentage of chert, ranging up to 44%. Within this cherty interval, reddish hues dominate and gray chert is absent. Review of shipboard-

F18. Chert distribution, thickness, percentage, and color trend, p. 30.

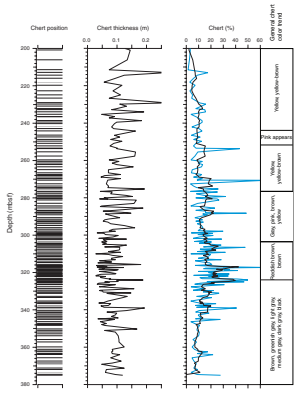

prepared thin sections of chert within, above, and below this interval show no apparent textural or compositional differences across this zone. It is somewhat unfortunate that because of logging difficulties at other sites and time constraints (Bralower, Premoli Silva, Malone et al., 2002), the most detailed analysis of chert distribution could only be made for Site 1207, where the downhole color patterns are least distinct (Fig. F19).

The major natural gamma radiation peaks in the logged sections at Sites 1207 and 1213 (Fig. F19) coincide with the occurrence of an Oceanic Anoxic Event (OAE1a) section (see discussion in Marsaglia, this volume), where the gamma signal is associated with uranium-rich organic matter (Bralower, Premoli Silva, Malone, et al., 2002). Elsewhere, where the gamma signal is less dependent on uranium/organic content, relative peaks are more likely controlled by the distribution of potassium- and thorium-rich clay minerals. Locally, clay-rich tuffaceous intervals occur below and above OAE1a (Marsaglia, this volume), but elsewhere in the section the clay may be wind-blown nonvolcanic dust. Although not pictured, the patterns in porosity and density logging measurements mimic those of resistivity and gamma ray logs pictured in Figure F19. There is a shallower high-resistivity zone at both sites (gray shading in Fig. F19), which is marked by five significant peaks in resistivity, density, and porosity. These were interpreted by shipboard scientists (Bralower, Premoli Silva, Malone, et al., 2002) as intervals of well-lithified sediment, possibly densely spaced chert beds. These correspond to red-brown chert intervals, which, at least at Site 1213, accumulated more slowly than adjacent gray chert intervals. Thin section, XRF, and XRD data from samples from this interval corroborate their high silica content.

F19. Downhole gamma radiation and resistivity logs, p. 31.

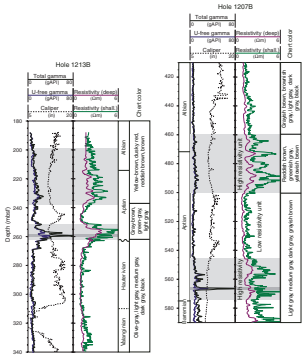

Differences in Patterns in Chert Color at Sites 1207 and 1213

Discrete downhole trends in color were documented at Sites 1213 and 1214, but a more mixed pattern was observed at Site 1207 (Figs. F2, F3, F4). As discussed above, there are major similarities between the electrical resistivity log profiles for Sites 1207 and 1213, located >600 km to the south. However, a bed-by-bed correlation is not possible. The greatest differences are noted in the Aptian Selli OAE1a interval, where variable organic matter and volcanic input may have had an effect (see Marsaglia, this volume). The general similarity of logging patterns at Sites 1207 and 1213 suggests that the length of Shatsky Rise was affected by variations in sedimentation style, and biostratigraphic data presented in Bralower, Premoli Silva, Malone, et al. (2002) indicate that there was more pronounced variability in sedimentation rate over the same intervals at the southern site.

DISCUSSION AND CONCLUSIONS

Shipboard scientists interpreted the secular color changes in Cretaceous chert as reflecting redox conditions, with the reddish hues tied to more oxidizing conditions and the gray hues tied to more reducing conditions (Bralower, Premoli Silva, Malone, et al., 2002). They also recognized this apparent trend at other DSDP sites (Leg 32, Sites 305 and 306) and hypothesized that the changing redox conditions were related to some combination of organic matter flux, sedimentation rate, and

deepwater oxygen level. Such changing conditions might have been recorded in the mineralogy, texture, or geochemistry of these rocks, and our goal was to see if we could identify these signals. We petrographically examined the transitions between calcareous and siliceous lithologies in many individual samples but remain uncertain as to whether textural and compositional variabilities present are the cause or the product of the chertification process. For example, diagenetic overprinting has likely greatly modified the amounts and relative proportions of siliceous and calcareous microfossils in these rocks. This makes any interpretation of the tendency for higher percentages of calcareous microfossils (foraminifers or ostracodes) in the red cherts somewhat equivocal. Does this tendency reflect greater sedimentation rates of these microfossils in the red chert intervals or preferential preservation? Bioturbation and lamination were more pronounced in the gray lithologies (chert/porcellanite), but again it is difficult to say whether this is real or an artifact of diagenesis. Thus our petrographic observations provide no concrete clues as to whether changes in environmental conditions produced the observed downhole color trends in chert.

Initially, we assumed that the chert color likely reflects the sediment color at the time of chert formation. This would imply that the reddish brown cherts formed under oxidizing conditions. We observed some examples where chert color (e.g., red = oxidized) did not correspond to the color of the surrounding host sediment (e.g., green limestone/porcellanite-reduced), suggesting postsilicification changes in oxidation state. Also, there are examples of variegated chert at the millimeter scale, suggesting changing oxidation states during diagenesis.

Element compositions were used to test whether there are significant and systematic differences among the varying chert colors. In general, the red cherts consist of >98 wt% silica with correspondingly low percentages of trace elements. The red chert color may simply be a function of the absence of other components, with red pigmentation produced by a small amount of iron oxides in a relatively pure silica groundmass. Gray and brown cherts appear to be much more variable in composition, and so their wide spectra are linked to combinations of contaminants including Fe, Mg, Mn, and Al (clay minerals), organic matter, phosphate, and carbonate. The chemistry of chert, porcellanite, and limestone from adjacent intact core provides some further hints on compositional relationships. For example, green chert color may be related to higher Mn content, and in brown chert, phosphate and/or organic matter may be the significant pigments. These results are not surprising in that we are analyzing the diagenetic aftermath of a process by which silica is segregated and concentrated in the sedimentary pile.

We attempted to relate chert petrology and geochemistry to the frequency and thickness of chert horizons as determined by downhole logging. Of the chert varieties, the reddish brown cherts are most distinct in that they correspond to intervals with greater percentages of chert, as well as distinct logging characteristics possibly tied to their very low porosity and high silica content. The similarity of logging character from the northern to the southern high suggests that there are regional patterns in silicification.

ACKNOWLEGMENTS

This work is part of a Master of Science thesis project by K. Fontilea at California State University Northridge (CSUN; USA). This research used

samples, data, and funding provided by the Ocean Drilling Program (ODP), which is sponsored by the U.S. National Science Foundation and participating countries under management of Joint Oceanographic Institutions (JOI), Inc. K.M. Marsaglia received additional funding from CSUN, and K. Fontilea received additional support from the Eisenhower Foundation.

REFERENCES

Bralower, T.J., Premoli Silva, I., Malone, M.J., et al., 2002. *Proc. ODP, Init. Repts.,* 198 [CD-ROM]. Available from: Ocean Drilling Program, Texas A&M University, College Station TX 77845-9547, USA.

Bramlette, M.N., 1946. The Monterey Formation of California and the origin of its siliceous rocks. *Geol. Surv. Prof. Pap. U.S.,* 212.

Douzen, K., and Ishiga, H., 1995. Changes of oceanic conditions at the Triassic/Jurassic boundary: sedimentary examination of bedded cherts of southwest Japan. *J. Geol. Soc. Jpn.,* 101:423–433.

Fraser, G.S., Harvey, R.D., and Heigold, P.C., 1972. Properties of chert related to its reactivity in an alkaline environment. *Circ.—Ill. State Geol. Surv.,* 468:31.

Hein, J.R., Vallier, T.L., and Allan, M.A., 1981. Chert petrology and geochemistry mid-Pacific Mountains and Hess Rise, Deep Sea Drilling Project Leg 62. *In* Thiede, J., Vallier, T.L., et al., *Init. Repts. DSDP,* 62: Washington (U.S. Govt. Printing Office), 711–748.

Hesse, R., 1990. Origin of chert: diagenesis of biogenic siliceous sediments. *In* McIlreath, I.A., and Morrow, D.W. (Eds.), *Diagenesis*. Geosci. Can. Repr. Ser., 4:227–251.

Ingamells, C.O., and Pitard, F.F., 1986. *Applied Geochemical Analysis:* New York (Wiley).

Isaacs, C.M., 1981a. Lithostratigraphy of the Monterey Formation, Goleta to Point Conception, Santa Barbara coast, California. *In* Isaacs, C.M. (Ed.), *Guide to the Monterey Formation in the California Coastal Area, Ventura to San Luis Obispo*. Pacific Sect. AAPG Field Guide, 52:9–23.

Isaacs, C.M., 1981b. Outline of diagenesis in the Monterey Formation examined laterally along the Santa Barbara coast, California. *In* Isaacs, C.M. (Ed.), *Guide to the Monterey Formation in the California Coastal Area, Ventura to San Luis Obispo*. Pacific Sect. AAPG Field Guide, 52:25–38.

Jones, D.L., and Murchey, B., 1986. Geological significance of Paleozoic and Mesozoic radiolarian chert. *Annu. Rev. Earth Planet. Sci.,* 14:455–492.

Keene, J.B., 1975. Cherts and porcellanites from the North Pacific DSDP, Leg 32. *In* Larson, R.L., Moberly, R., et al. *Init. Repts. DSDP,* 32: Washington (U.S. Govt. Printing Office), 429–507.

Luedtke, B.E., 1978. Chert sources and trace element analysis. *Am. Antiq.,* 43:413–423.

Pisciotto, K.A., 1980. Chert and porcellanite from Deep Sea Drilling Project Site 43, northwest Pacific. *In* Scientific Party, *Init. Repts. DSDP,* 56, 57, Pt. 2: Washington (U.S. Govt. Printing Office), 1133–1142.

Ragland, P.C., 1989. *Basic Analytical Petrology:* New York (Oxford Univ. Press).

Rock-Color Chart Committee, 1991. *Rock Color Charts:* Boulder (Geol. Soc. Am.).

Figure F1. Location map showing a perspective topography of Shatsky Rise and Leg 198 site locations from Bralower, Premoli Silva, Malone. et al. (2002).

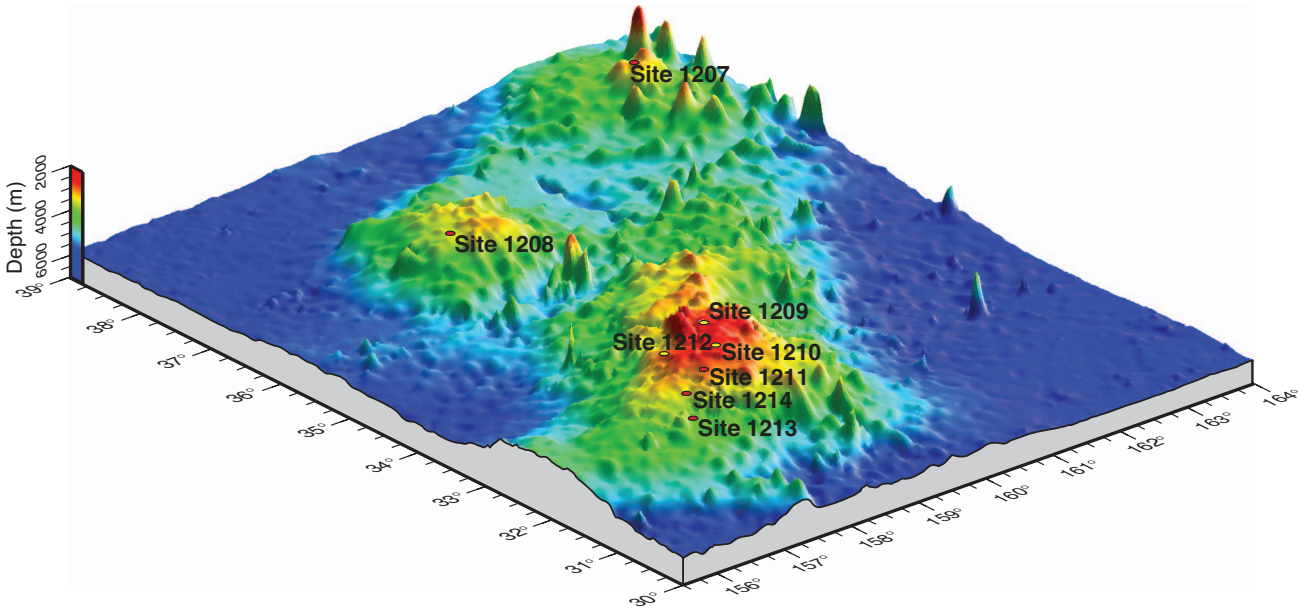

Figure F2. Downhole variations in colors of chert recovered from Hole 1207B from Bralower, Premoli Silva, Malone. et al. (2002).

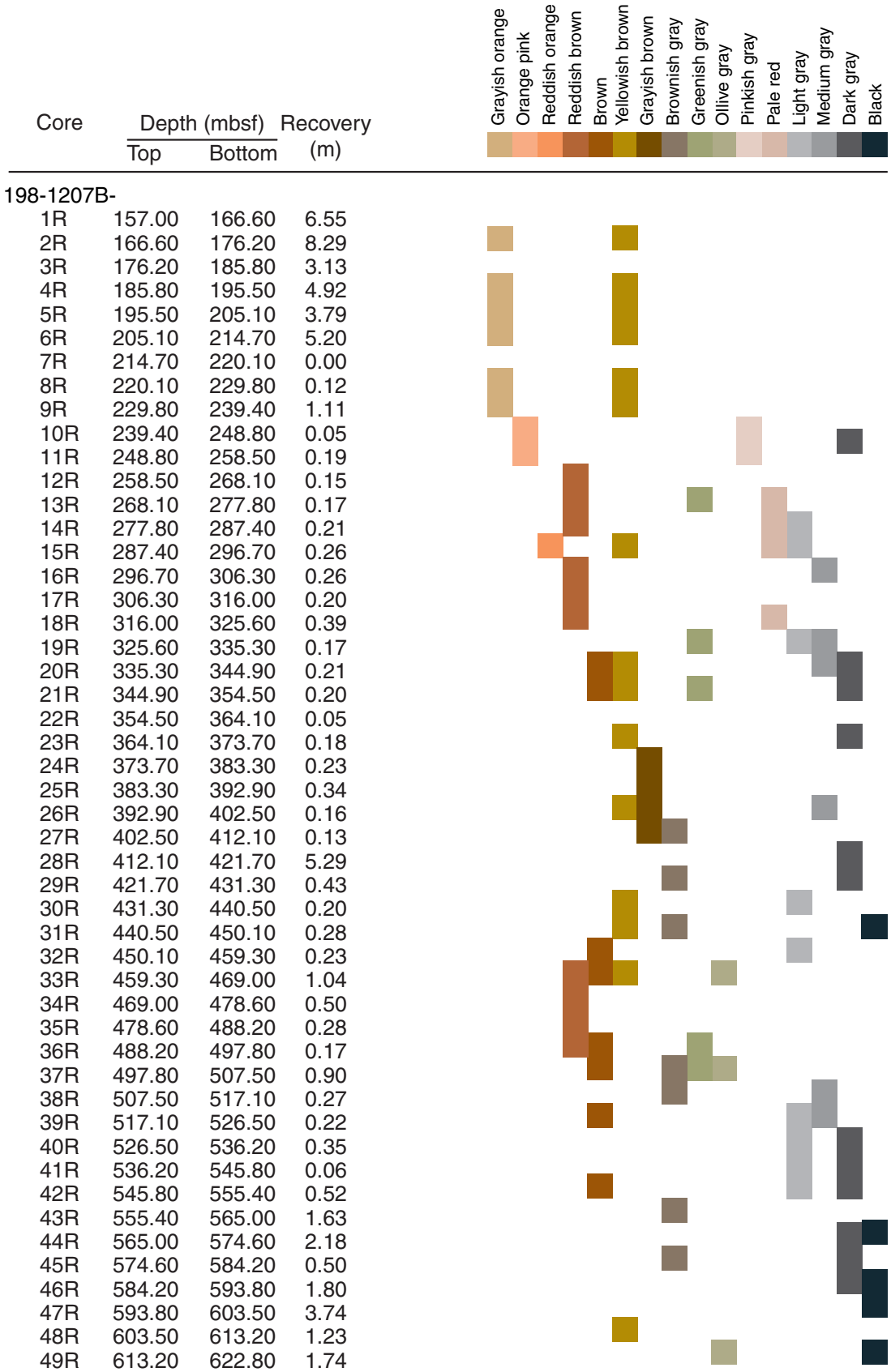

Core	Depth (mbsf) Top	Depth (mbsf) Bottom	Recovery (m)
198-1207B-			
1R	157.00	166.60	6.55
2R	166.60	176.20	8.29
3R	176.20	185.80	3.13
4R	185.80	195.50	4.92
5R	195.50	205.10	3.79
6R	205.10	214.70	5.20
7R	214.70	220.10	0.00
8R	220.10	229.80	0.12
9R	229.80	239.40	1.11
10R	239.40	248.80	0.05
11R	248.80	258.50	0.19
12R	258.50	268.10	0.15
13R	268.10	277.80	0.17
14R	277.80	287.40	0.21
15R	287.40	296.70	0.26
16R	296.70	306.30	0.26
17R	306.30	316.00	0.20
18R	316.00	325.60	0.39
19R	325.60	335.30	0.17
20R	335.30	344.90	0.21
21R	344.90	354.50	0.20
22R	354.50	364.10	0.05
23R	364.10	373.70	0.18
24R	373.70	383.30	0.23
25R	383.30	392.90	0.34
26R	392.90	402.50	0.16
27R	402.50	412.10	0.13
28R	412.10	421.70	5.29
29R	421.70	431.30	0.43
30R	431.30	440.50	0.20
31R	440.50	450.10	0.28
32R	450.10	459.30	0.23
33R	459.30	469.00	1.04
34R	469.00	478.60	0.50
35R	478.60	488.20	0.28
36R	488.20	497.80	0.17
37R	497.80	507.50	0.90
38R	507.50	517.10	0.27
39R	517.10	526.50	0.22
40R	526.50	536.20	0.35
41R	536.20	545.80	0.06
42R	545.80	555.40	0.52
43R	555.40	565.00	1.63
44R	565.00	574.60	2.18
45R	574.60	584.20	0.50
46R	584.20	593.80	1.80
47R	593.80	603.50	3.74
48R	603.50	613.20	1.23
49R	613.20	622.80	1.74

Figure F3. Downhole variations in colors of chert recovered from Site 1213 from Bralower, Premoli Silva, Malone. et al. (2002).

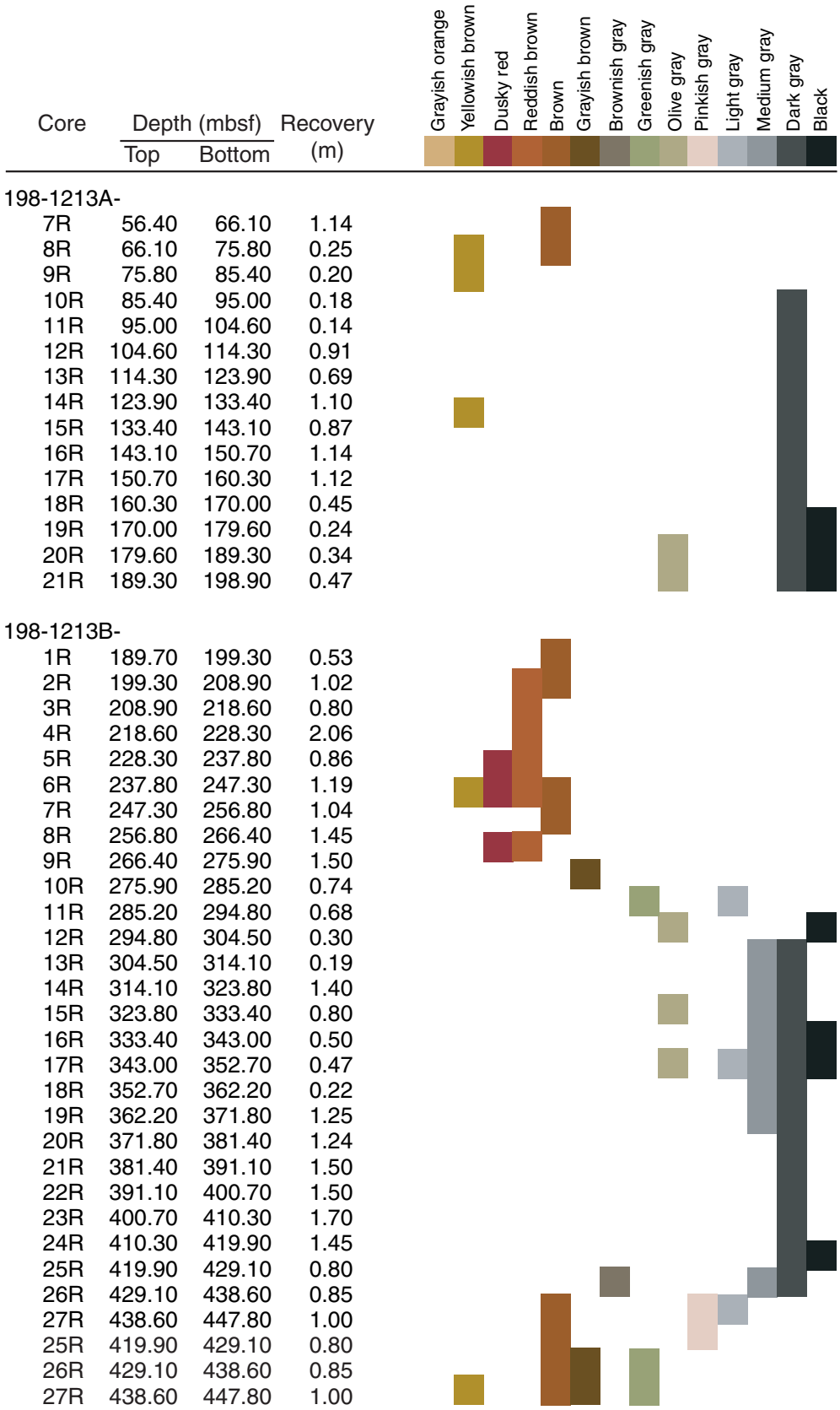

Core	Depth (mbsf) Top	Depth (mbsf) Bottom	Recovery (m)
198-1213A-			
7R	56.40	66.10	1.14
8R	66.10	75.80	0.25
9R	75.80	85.40	0.20
10R	85.40	95.00	0.18
11R	95.00	104.60	0.14
12R	104.60	114.30	0.91
13R	114.30	123.90	0.69
14R	123.90	133.40	1.10
15R	133.40	143.10	0.87
16R	143.10	150.70	1.14
17R	150.70	160.30	1.12
18R	160.30	170.00	0.45
19R	170.00	179.60	0.24
20R	179.60	189.30	0.34
21R	189.30	198.90	0.47
198-1213B-			
1R	189.70	199.30	0.53
2R	199.30	208.90	1.02
3R	208.90	218.60	0.80
4R	218.60	228.30	2.06
5R	228.30	237.80	0.86
6R	237.80	247.30	1.19
7R	247.30	256.80	1.04
8R	256.80	266.40	1.45
9R	266.40	275.90	1.50
10R	275.90	285.20	0.74
11R	285.20	294.80	0.68
12R	294.80	304.50	0.30
13R	304.50	314.10	0.19
14R	314.10	323.80	1.40
15R	323.80	333.40	0.80
16R	333.40	343.00	0.50
17R	343.00	352.70	0.47
18R	352.70	362.20	0.22
19R	362.20	371.80	1.25
20R	371.80	381.40	1.24
21R	381.40	391.10	1.50
22R	391.10	400.70	1.50
23R	400.70	410.30	1.70
24R	410.30	419.90	1.45
25R	419.90	429.10	0.80
26R	429.10	438.60	0.85
27R	438.60	447.80	1.00
25R	419.90	429.10	0.80
26R	429.10	438.60	0.85
27R	438.60	447.80	1.00

Figure F4. Downhole variations in colors of chert recovered from Hole 1214A from Bralower, Premoli Silva, Malone. et al. (2002).

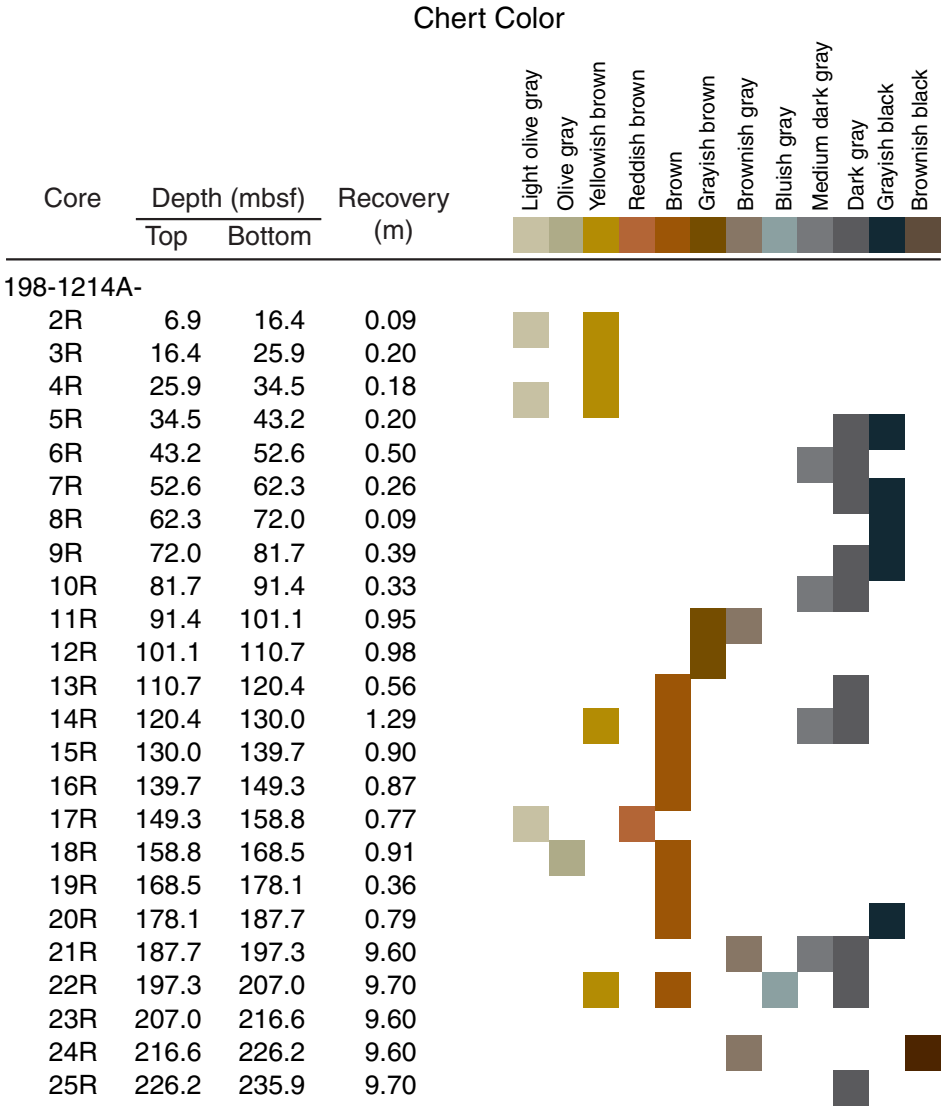

Core	Depth (mbsf) Top	Depth (mbsf) Bottom	Recovery (m)
198-1214A-			
2R	6.9	16.4	0.09
3R	16.4	25.9	0.20
4R	25.9	34.5	0.18
5R	34.5	43.2	0.20
6R	43.2	52.6	0.50
7R	52.6	62.3	0.26
8R	62.3	72.0	0.09
9R	72.0	81.7	0.39
10R	81.7	91.4	0.33
11R	91.4	101.1	0.95
12R	101.1	110.7	0.98
13R	110.7	120.4	0.56
14R	120.4	130.0	1.29
15R	130.0	139.7	0.90
16R	139.7	149.3	0.87
17R	149.3	158.8	0.77
18R	158.8	168.5	0.91
19R	168.5	178.1	0.36
20R	178.1	187.7	0.79
21R	187.7	197.3	9.60
22R	197.3	207.0	9.70
23R	207.0	216.6	9.60
24R	216.6	226.2	9.60
25R	226.2	235.9	9.70

Figure F5. Downhole variations in colors of chert recovered from Hole 1207B, revised from Bralower, Premoli Silva, Malone. et al. (2002), after further description.

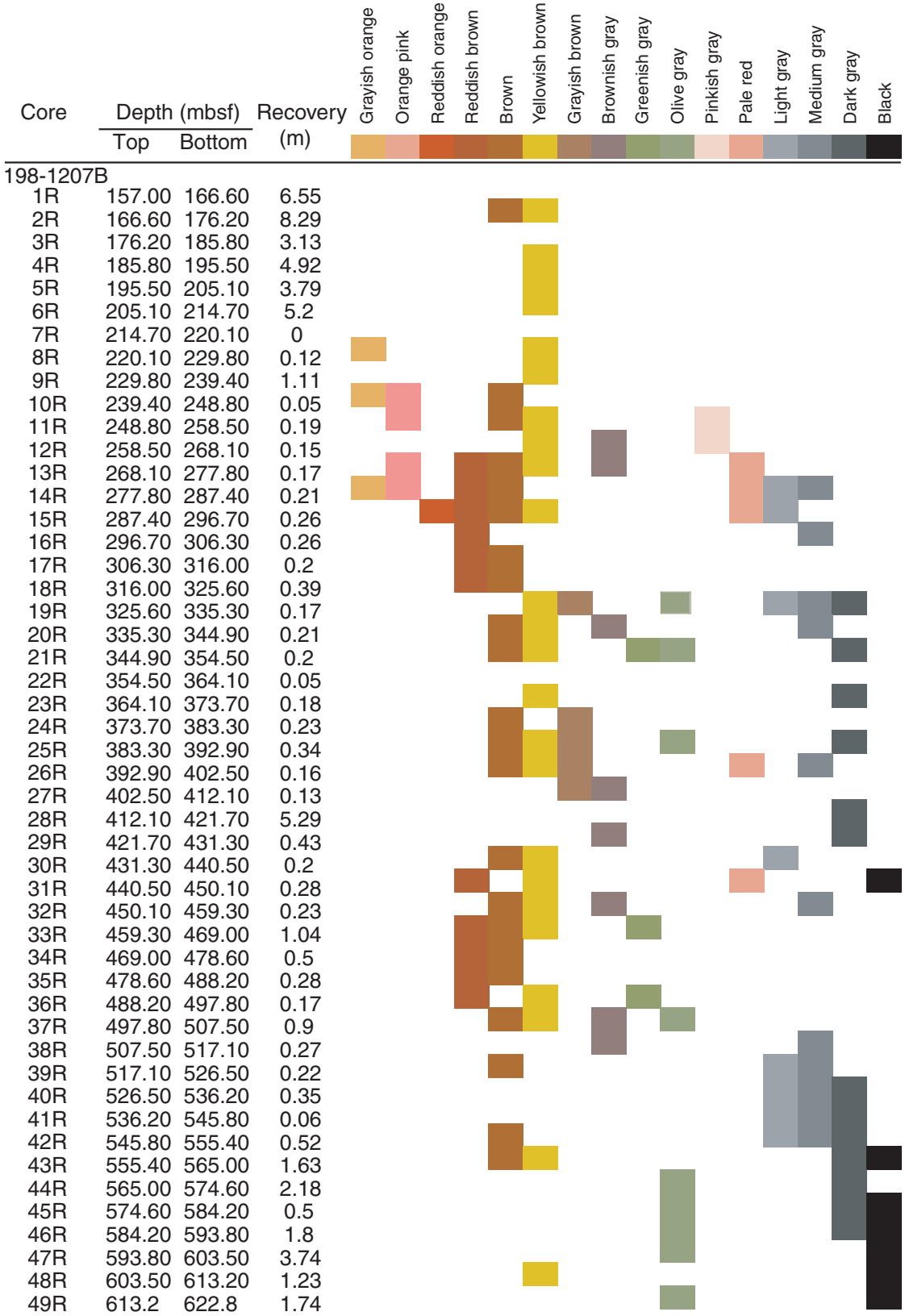

Core	Depth (mbsf) Top	Depth (mbsf) Bottom	Recovery (m)
198-1207B			
1R	157.00	166.60	6.55
2R	166.60	176.20	8.29
3R	176.20	185.80	3.13
4R	185.80	195.50	4.92
5R	195.50	205.10	3.79
6R	205.10	214.70	5.2
7R	214.70	220.10	0
8R	220.10	229.80	0.12
9R	229.80	239.40	1.11
10R	239.40	248.80	0.05
11R	248.80	258.50	0.19
12R	258.50	268.10	0.15
13R	268.10	277.80	0.17
14R	277.80	287.40	0.21
15R	287.40	296.70	0.26
16R	296.70	306.30	0.26
17R	306.30	316.00	0.2
18R	316.00	325.60	0.39
19R	325.60	335.30	0.17
20R	335.30	344.90	0.21
21R	344.90	354.50	0.2
22R	354.50	364.10	0.05
23R	364.10	373.70	0.18
24R	373.70	383.30	0.23
25R	383.30	392.90	0.34
26R	392.90	402.50	0.16
27R	402.50	412.10	0.13
28R	412.10	421.70	5.29
29R	421.70	431.30	0.43
30R	431.30	440.50	0.2
31R	440.50	450.10	0.28
32R	450.10	459.30	0.23
33R	459.30	469.00	1.04
34R	469.00	478.60	0.5
35R	478.60	488.20	0.28
36R	488.20	497.80	0.17
37R	497.80	507.50	0.9
38R	507.50	517.10	0.27
39R	517.10	526.50	0.22
40R	526.50	536.20	0.35
41R	536.20	545.80	0.06
42R	545.80	555.40	0.52
43R	555.40	565.00	1.63
44R	565.00	574.60	2.18
45R	574.60	584.20	0.5
46R	584.20	593.80	1.8
47R	593.80	603.50	3.74
48R	603.50	613.20	1.23
49R	613.2	622.8	1.74

Figure F6. Lithostratigraphy at Sites 1207, 1213, and 1214 showing sample intervals and types of analyses (thin section, XRF) performed. Color column is provided to indicate intervals of predominantly gray and dark gray cherts (black) vs. intervals where chert is predominantly reddish brown (white). Modified from Bralower, Premoli Silva, Malone. et al. (2002). TD = total depth.

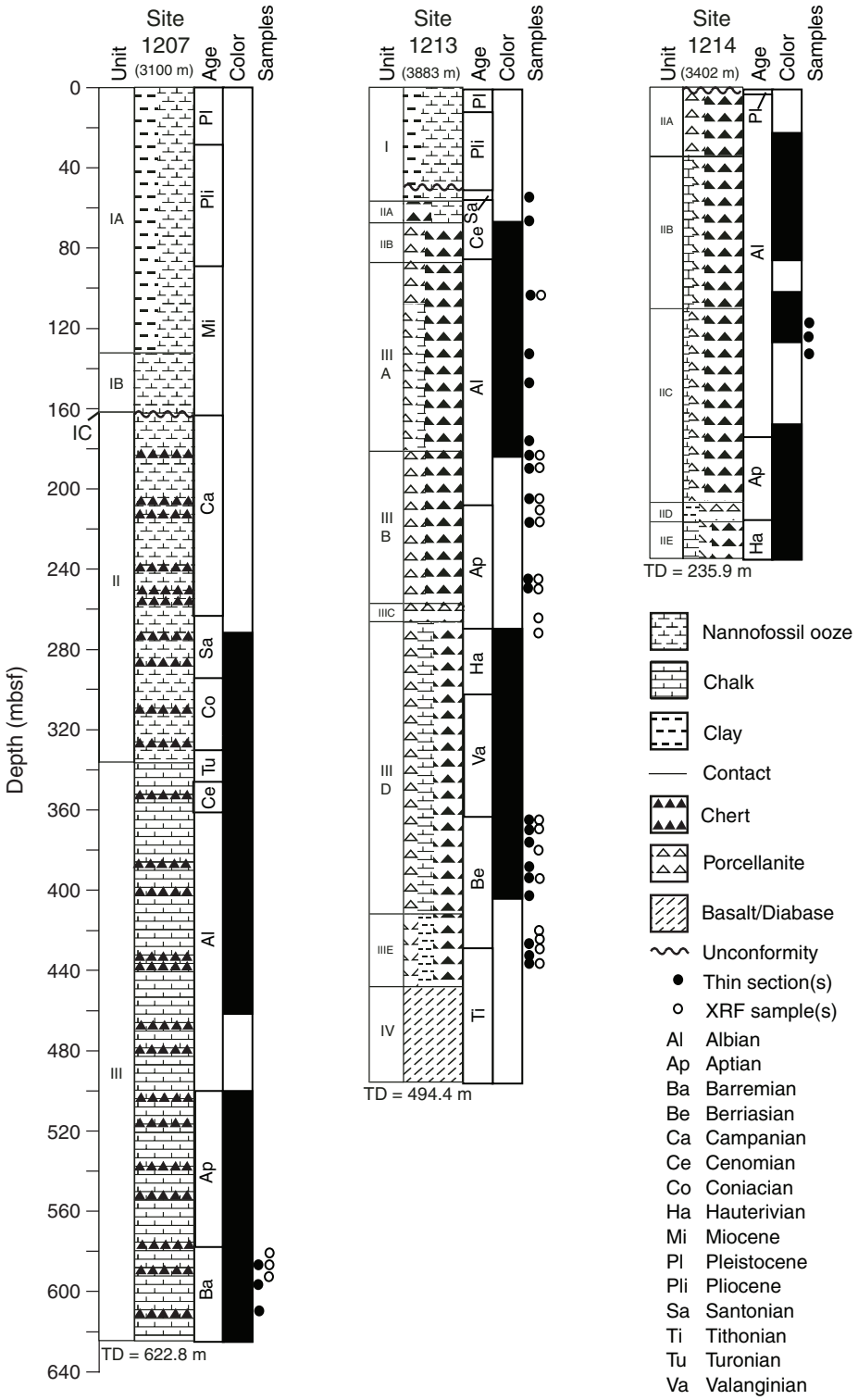

Figure F7. Normalized percentages of SiO_2 and CaO for chert, mixed, and limestone samples. Mixed lithologies are as indicated (see Table T6, p. 45). XRF = X-ray fluorescence.

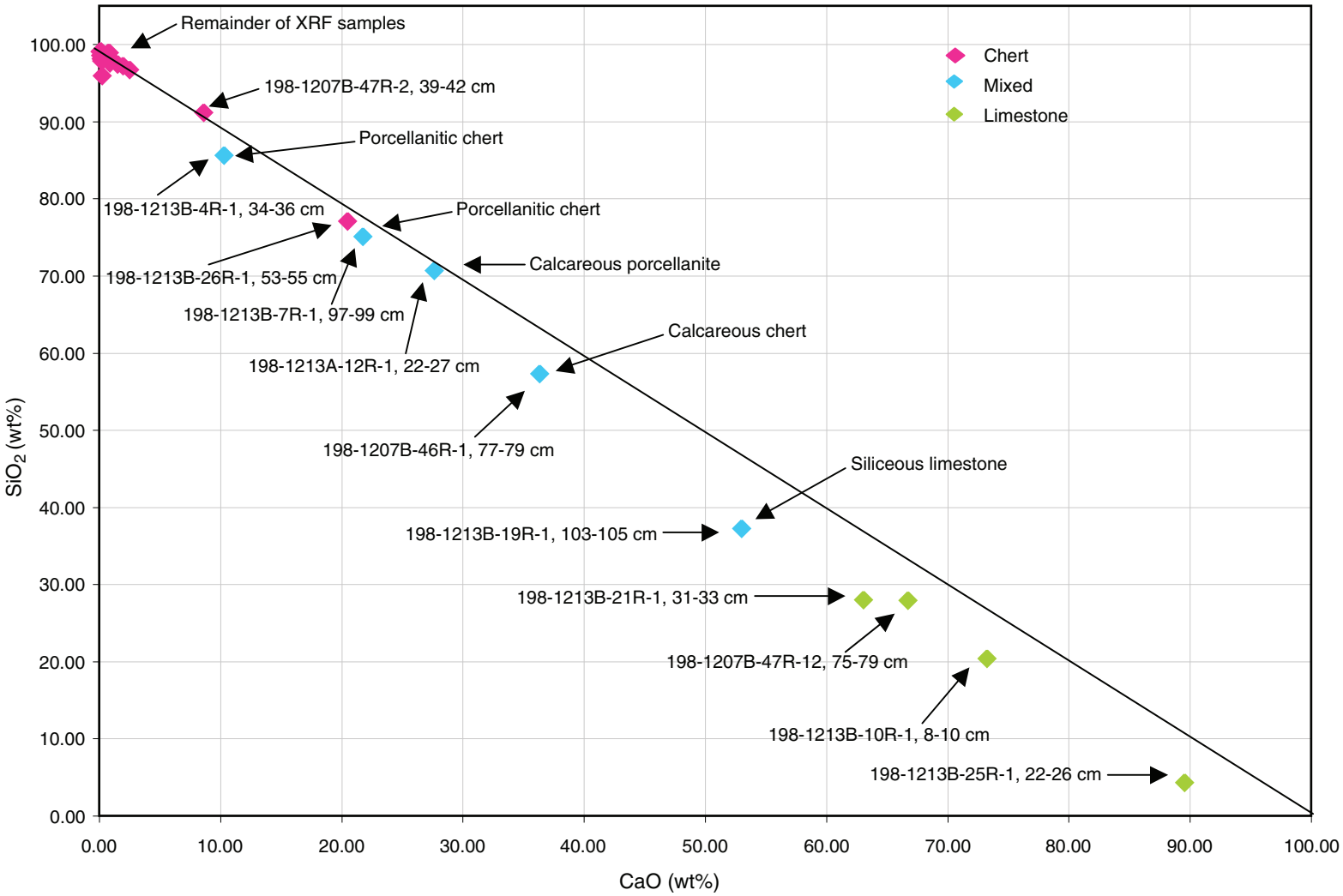

Figure F8. Concentration of barium in XRF samples. Note that porcellanite category includes porcellanitic lithologies.

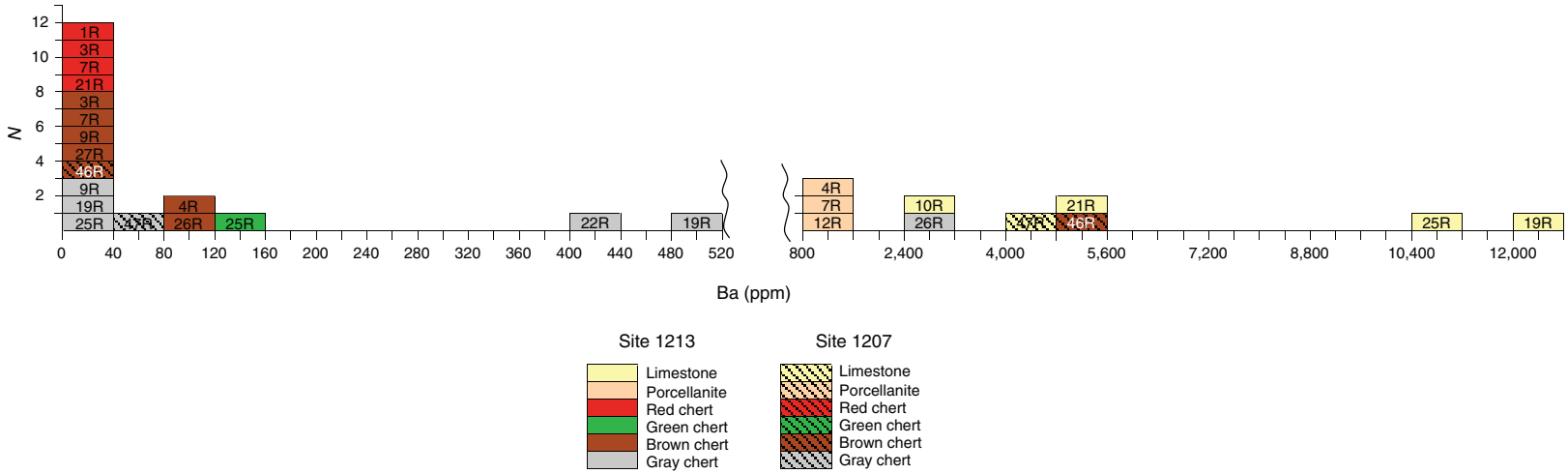

Figure F9. Concentration of strontium in XRF samples. Note that porcellanite category includes porcellanitic lithologies.

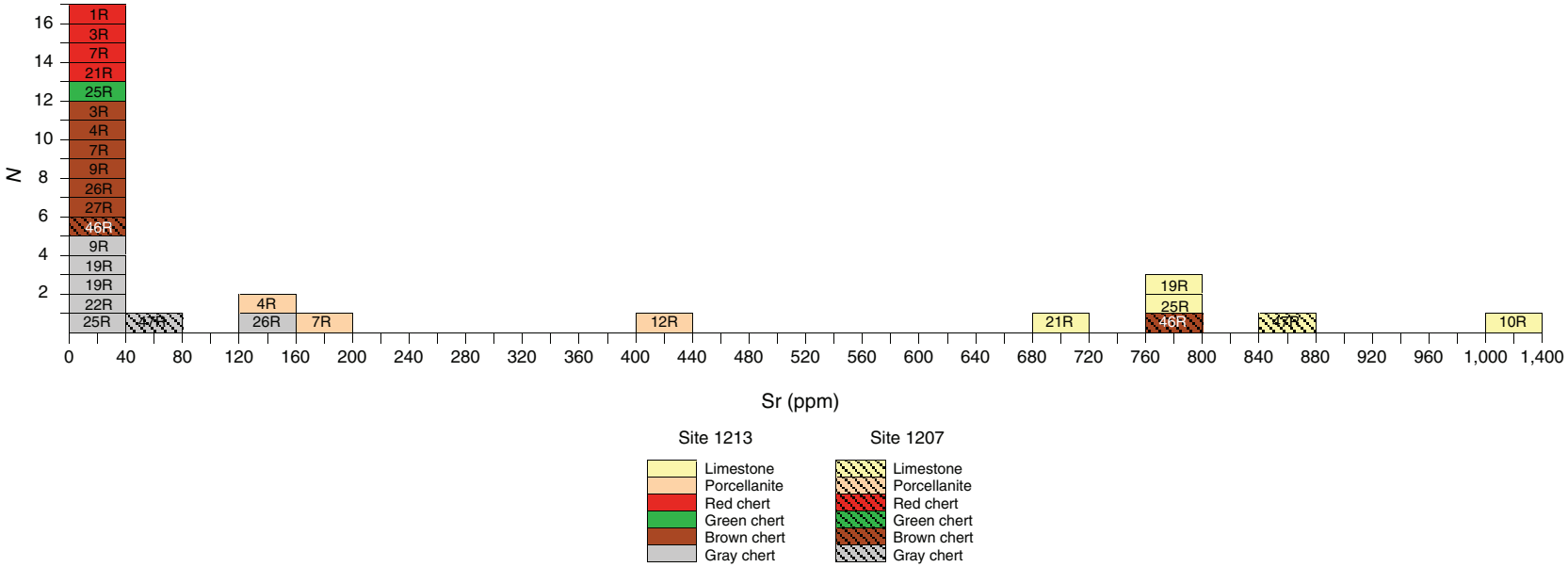

Figure F10. Concentration of titanium in XRF samples. Note that porcellanite category includes porcellanitic lithologies.

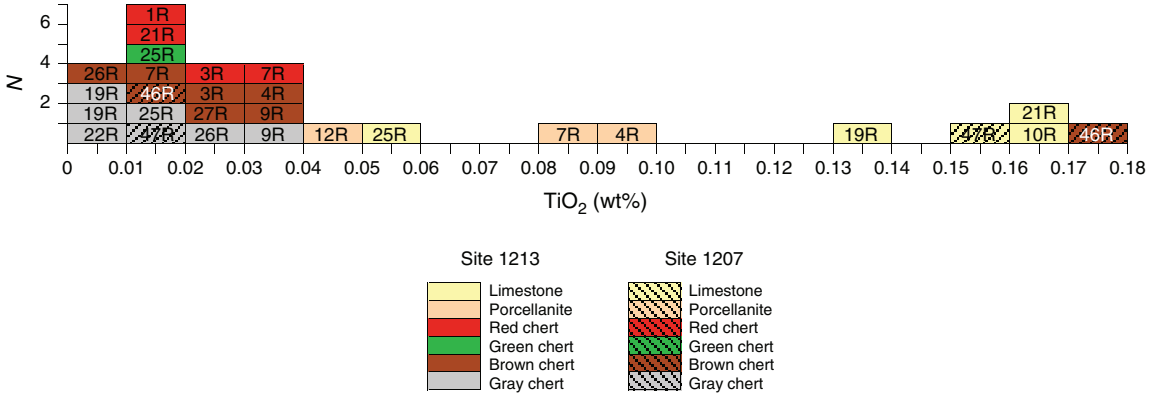

Figure F11. Concentration of aluminum in XRF samples. Note that porcellanite category includes porcellanitic lithologies.

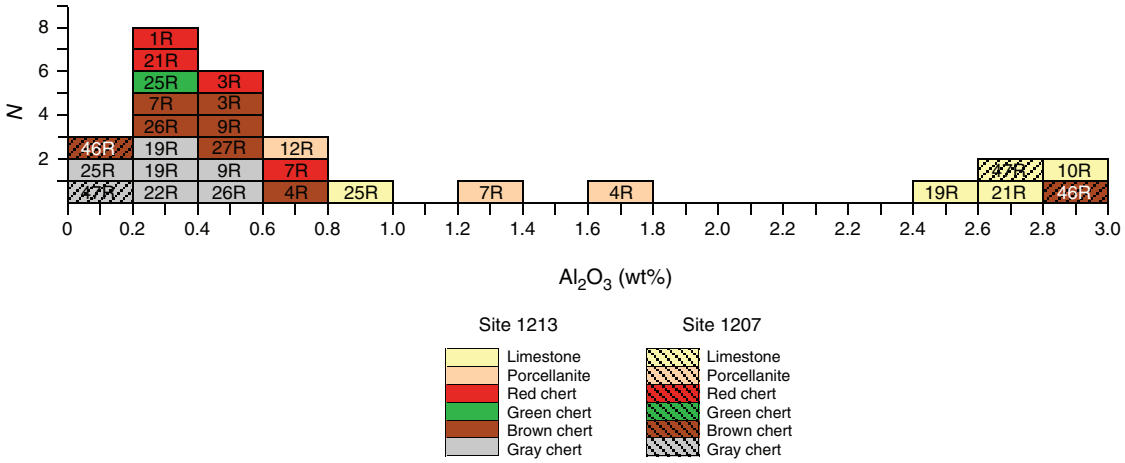

Figure F12. Concentration of magnesium in XRF samples. Note that porcellanite category includes porcellanitic lithologies.

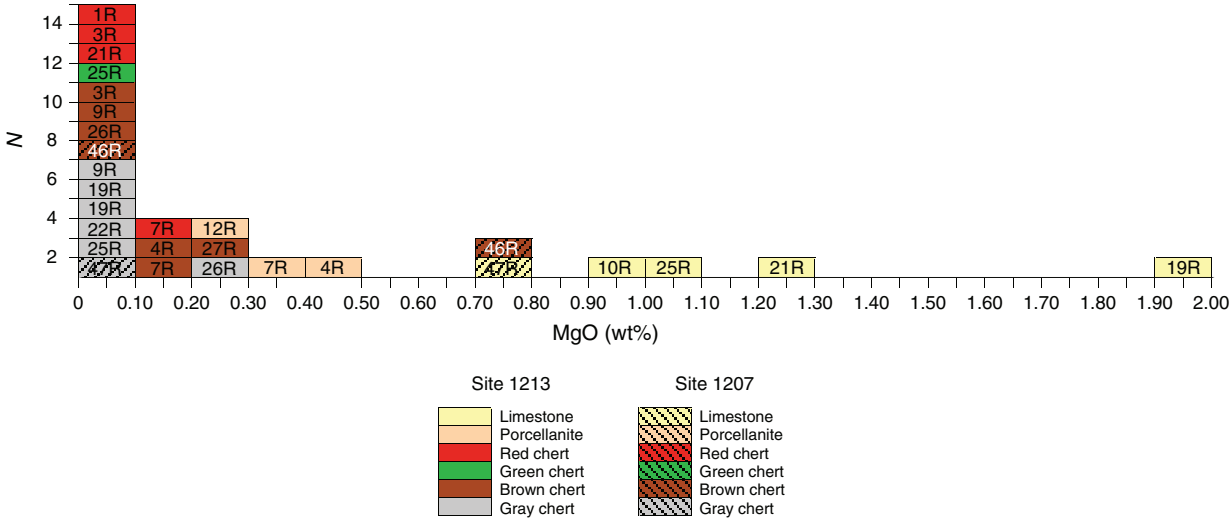

Figure F13. Concentration of potassium in XRF samples. Note that porcellanite category includes porcellanitic lithologies.

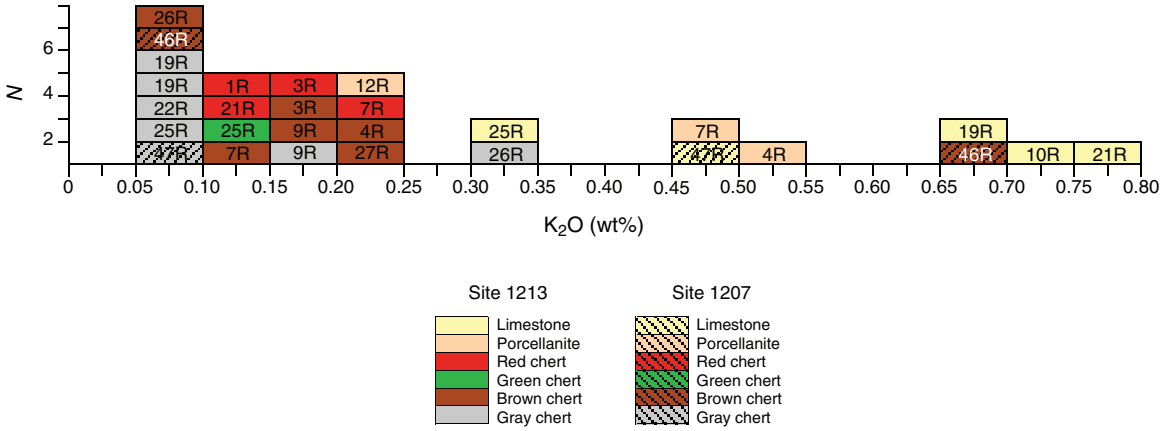

Figure F14. Concentration of iron in XRF samples. Note that porcellanite category includes porcellanitic lithologies.

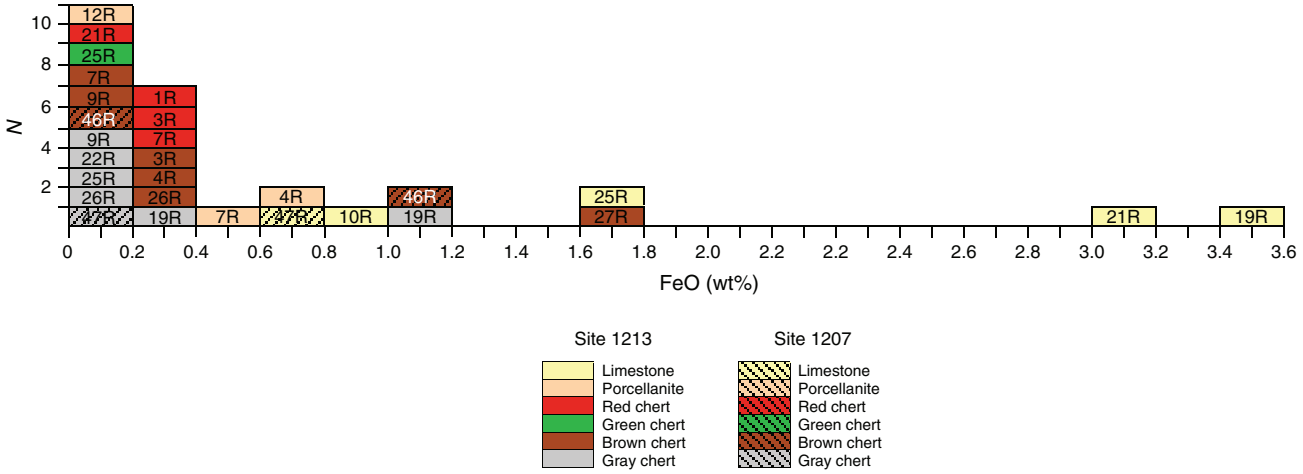

Figure F15. Concentration of manganese in XRF samples. Note that porcellanite category includes porcellanitic lithologies.

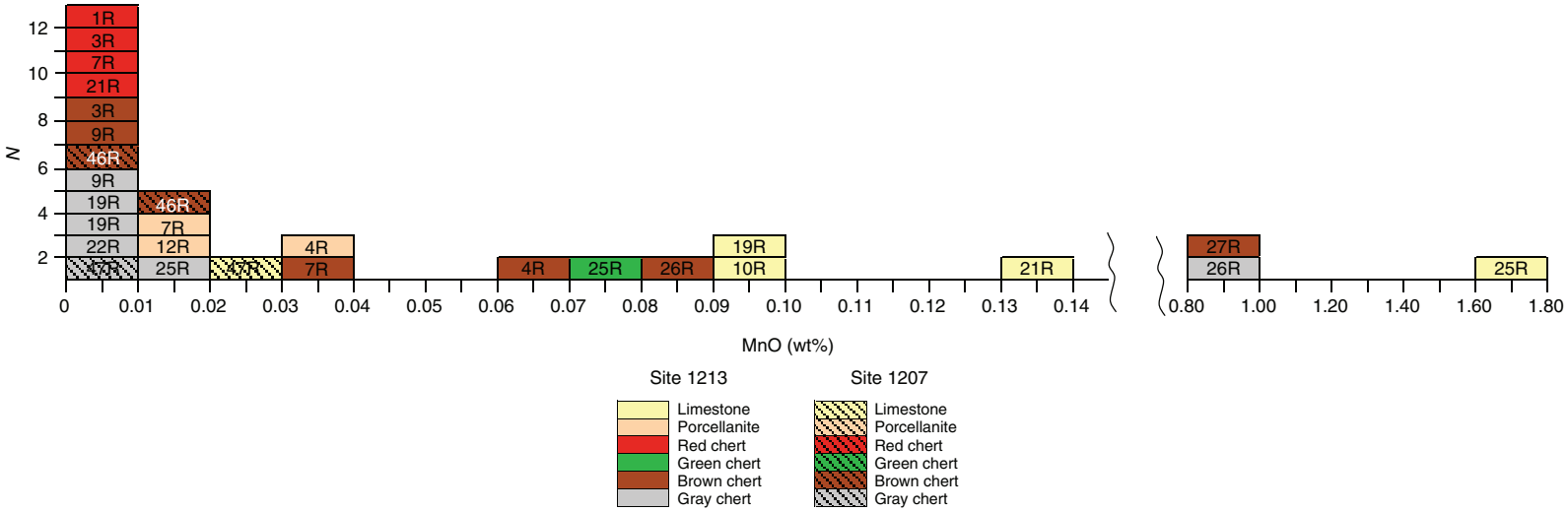

Figure F16. Concentration of phosphorus in XRF samples. Note that porcellanite category includes porcellanitic lithologies.

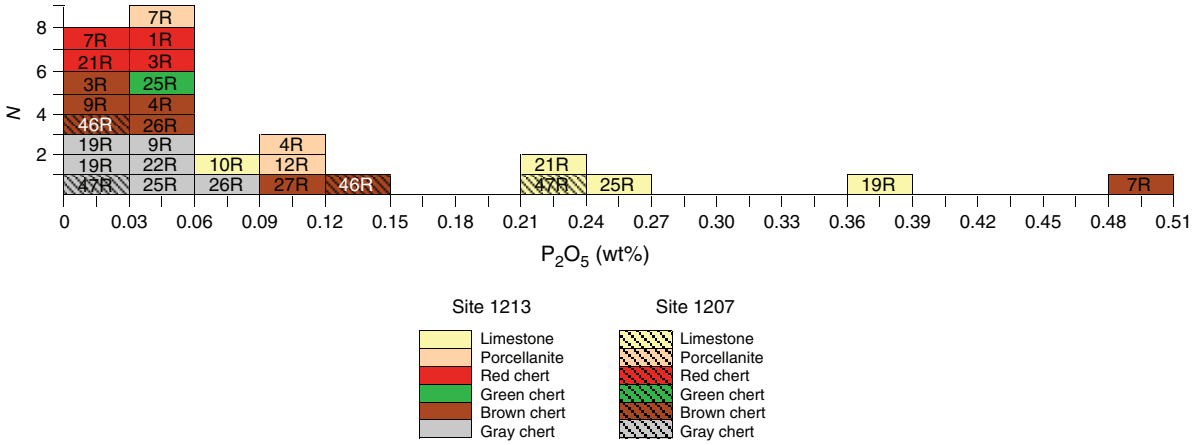

Figure F17. Concentration of sodium in XRF samples. Note that porcellanite category includes porcellanitic lithologies.

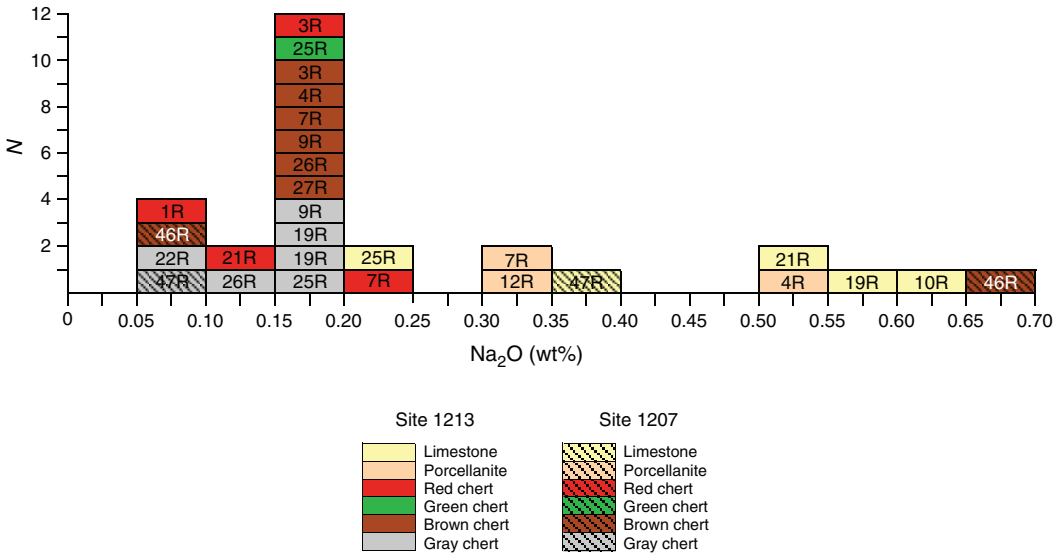

Figure F18. Chert distribution, thickness, percentage, and color trend for Hole 1207B. Modified from Bralower, Premoli Silva, Malone, et al. (2002).

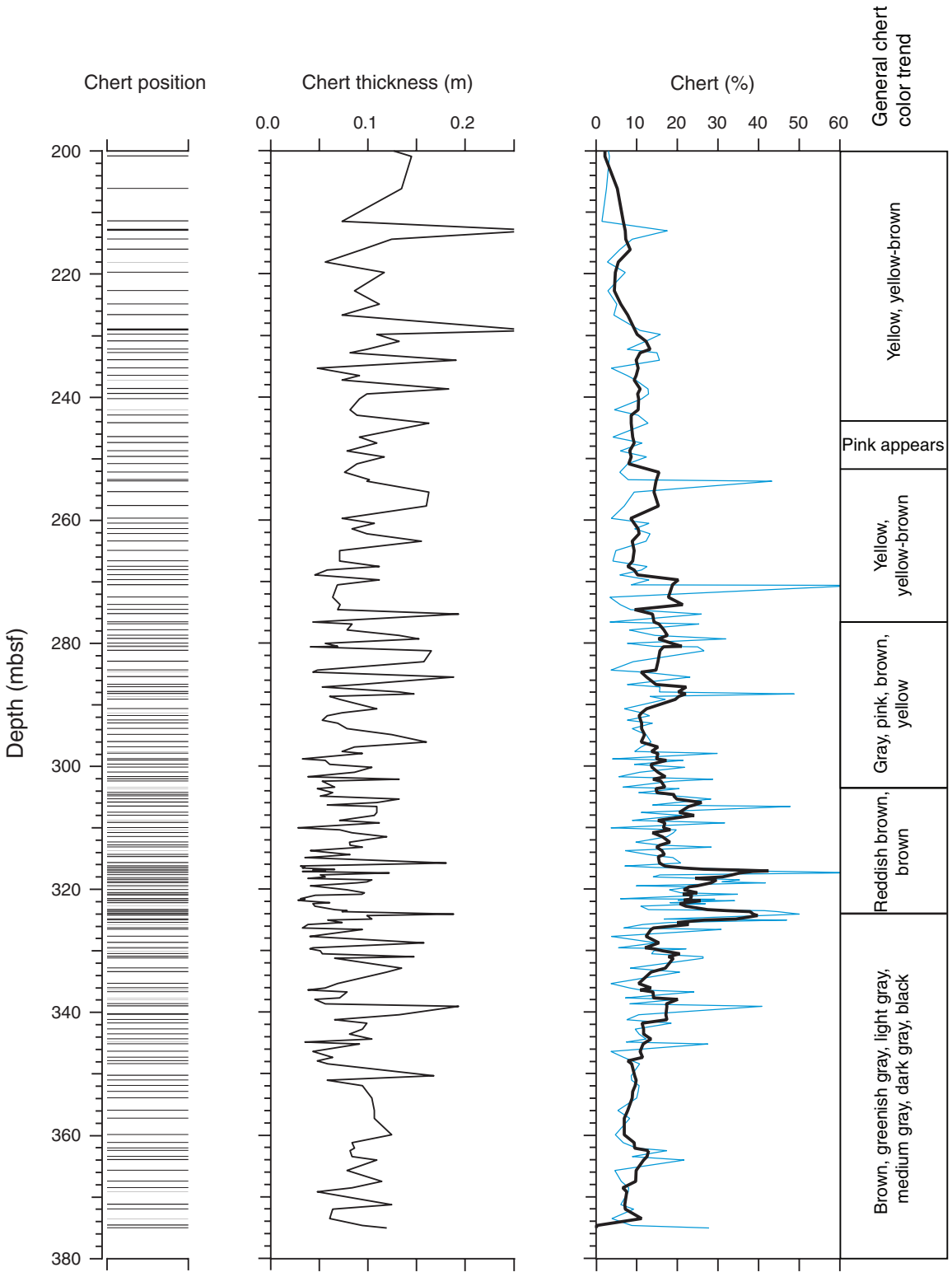

Figure F19. Downhole gamma radiation and resistivity logs and general chert colors (see Figs. F2, p. 14, F3, p. 15, F4, p. 16, and F5, p. 17) for Holes 1207B and 1213B. Modified from Bralower, Premoli Silva, Malone, et al. (2002). shall. = shallow.

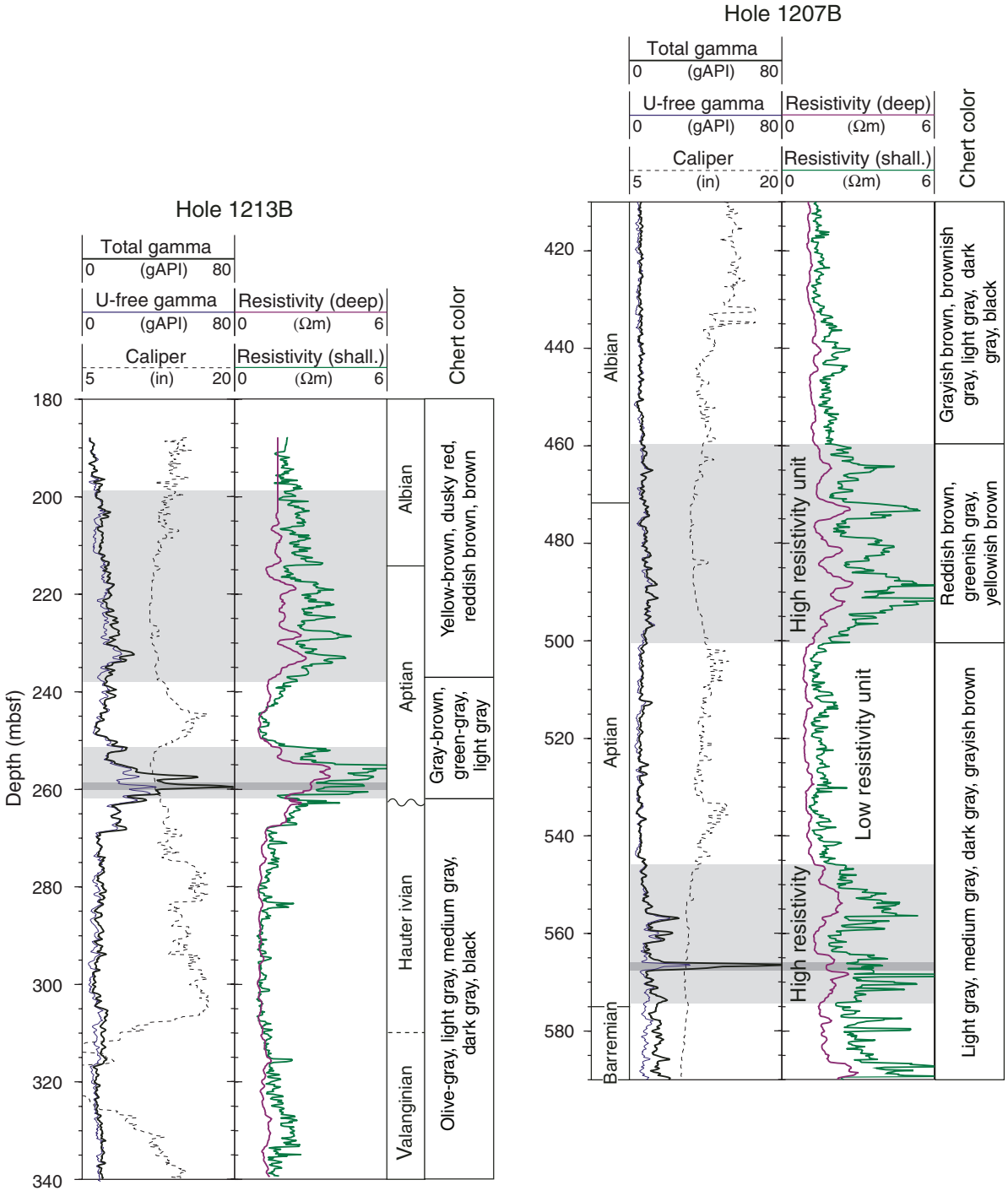

Table T1. Summary of studies relating chert color to trace element composition.

Source article	Techniques (elements analyzed)	Age of chert	Location	Chert color range	Summary of results
Leudtke (1978)	INAA (Sm, Yb, Lu, La, Np/U, Sc, Na, Br, Ce, Th/P, Cr, Hf, Ba, Cs, Co, Rb, Eu, Sb, and Fe)	early Mississippian	Oceana County, Michigan	Gray to brown	1. Gray chalcedony had smaller proportions of all analyzed elements, except uranium and bromine. 2. Sandy brown chert had the greatest proportions of all elements, except uranium and bromine. 3. Gray chert is intermediate for all elements. 4. Chemical variations can exist within formations.
Frasier et al. (1972)	Flame AAS (Na_2O and K_2O)	late Cambrian to Mississippian	Illinois: Union County, Johnson County, Alexander County, Hardin County, McDonough County, Brown County, Kankakee County, Adams County	Black to gray to brown	1. Chemical composition varied mainly in the relative amounts of SiO_2 and CaO.
	XRF (TiO_2, Al_2O_3, Fe_2O_3, MnO, MgO)		Nevada: Hardin County California: San Francisco (Twin Peaks) Montana: Granite County, Near Old Mines Ohio: Flint Ridge Park Indiana: near Veedersburg		
Hein et al. (1975)	X-ray mineralogy (quartz, calcite, smectite, hematite, illite, feldspar, barite, anhydrite, chlorite, apatite, gypsum)	early Cretaceous to early Pliocene	Deep Sea Drilling Project Leg 62: Central North Pacific Ocean, Mid-Pacific Mountains, Hess Rise	Orange to brown to gray to black	1. The carbonate component of the chert is distinguished by high values of MgO, CaO, Mn, Ba, Sr, and Zr.
	XRF (Mn, Ba, B, Zn, Ni, Y, Zn, Cu, Mo, Cr, Cu, SiO_2, CaO, Al_2O_3, Fe_2O_3, CaO, Na_2O, K_2O, MgO)				2. Tuffaceous cherts have high values of K and Al, and commonly Zn, Mo, and Cr. 3. Pure cherts are characterized by high SiO_2 and B. 4. High B percentages may be a good indication that the chert formed in an open-marine environment, isolated from terrigenous materials.

Notes: INAA = instrumental neutron activation analysis, AAS = atomic absorption spectroscopy, XRF = X-ray fluorescence.

Table T2. Hand specimen descriptions including age, lithology, and color. (**See table notes.** Continued on next four pages.)

Core, section, interval (cm)	Depth (mbsf)	Age (Ma)	Time period	Lithology	Colors		
					Chert	Porcellanite	Limestone
198-1213A-							
7R-CC, 0–3	57.31–57.34	85	Turonian	Chert and porcellanite	Dusky yellow brown (10YR 2/2) to moderate brown (5YR 4/4) and minor pale yellowish brown (10YR 6/2)	Very pale orange (10YR 8/2)	
8R-CC, 9–12	66.19–66.22	95	Cenomian	Chert and porcellanite	Dark yellowish orange (10YR 6/6), moderate reddish orange (10R 6/6), moderate reddish brown (10R 4/6), moderate orangish pink (10R 7/4) and pale yellowish orange (10YR 8/6)	Minor: white (N9)	
8R-CC, 12–15	66.22–66.25	95	Cenomian	Porcellanite and chert	Minor: moderate yellowish brown (10YR 5/4)	Yellowish gray (5Y 8/1)	
12R-1, 22–27	104.82–104.87	103	Cenomian	Porcellanite and chert	Minor: olive-black (5Y 2/1)	Yellowish gray (5Y 8/1)	
12R-1, 36–40	104.96–105.00	103	Cenomian	Chert, porcellanite, and limestone (?)	Dark gray (N3)	Yellowish gray (5Y 8/1)	Yellowish gray (5Y 8/1)
15R-1, 64–67	134.04–134.07	104	Cenomian	Porcellanite and chert	Minor: dusky yellowish brown (10YR 2/2)	Light gray (N8)	
15R-1, 77–80	134.17–134.20	104	Cenomian	Chert and porcellanite	Olive-black (5Y 2/1), minor burrows	Yellowish gray (5Y 8/1)	
16R-1, 101–104	144.11–144.14	105	Cenomian	Chert and porcellanite	Olive-black (5Y 2/1), minor burrows	Very light gray (N8) and yellowish gray (5Y 8/1)	
20R-1, 5–10	179.65–179.70	106	Albian	Chert and porcellanite	Moderate brown (5YR 4/4), with minor porcellanite filled burrows	Yellowish gray (5Y 8/1)	
21R-1, 36–40	189.66–189.70	115	Albian	Chert and porcellanite	Moderate brown (5YR 4/4), with minor porcellanite filled burrows	Yellowish gray (5Y 8/1)	
198-1213B-							
1R-1, 28–30	189.98–190.00	105	Albian	Chert	Moderate brown (5YR 4/4) and pale yellowish brown (10YR 6/2)		
1R-1, 52–54	190.22–190.24	105	Albian	Chert	Moderate brown (5YR 4/4), minor moderate reddish brown (10R 4/6), minor blackish red (5R 2/2)		
1R-1, 57–59	190.27–190.29	105	Albian	Chert	Moderate reddish brown (10R 4/6), minor moderate orange pink (10R 7/4)		
2R-1, 2–4	199.32–199.34	108	Albian	Chert and porcellantie	Dark reddish brown (10R 3/4)	Very pale orange (10YR 8/2)	
2R-1, 29–30	199.59–199.60	108	Albian	Chert and porcellanite	Mostly dark reddish brown (10R 3/4), minor moderate reddish brown (10R 4/6)	Minor: moderate orange pink (5YR 8/4) on edge	
2R-1, 59–61	199.89–199.91	108	Albian	Chert	Moderate reddish brown (10R 4/6), minor moderate reddish orange (10R 6/6) in burrows		
3R-1, 41–43	209.31–209.33	115	Albian	Chert and porcellanite	Dark reddish brown (10R 3/4), minor moderate reddish orange (10R 6/6)	Very pale orange (10YR 8/2)	
3R-1, 53–55	209.43–209.45	115	Albian	Chert and porcellanite	Moderate reddish brown (10R 4/6) and moderate brown (5YR 4/4), with black (N1) laminations	Minor: moderate orange pink (5YR 8/4)	
3R-1, 73–75	209.63–209.65	115	Albian	Chert and porcellanite	Moderate brown (5YR 3/4) with patches of moderate reddish brown (10R 4/6)	Moderate orange pink (10R 7/4) and pale red (10R 6/2) in few burrows, very pale orange (10YR 8/2) and moderate orange pink (5YR 8/4) porcellanite on edges	
4R-2, 2–3	220.12–220.13	117	Albian	Porcellanite	Mostly moderate yellowish brown (10YR 5/4) with minor light brown (5YR 6/4) laminations (?)		

Table T2 (continued).

Core, section, interval (cm)	Depth (mbsf)	Age (Ma)	Time period	Lithology	Colors		
					Chert	Porcellanite	Limestone
4R-2, 6–8	220.16–220.18	117	Albian	Porcellanite	Mostly moderate yellowish brown (10YR 5/4)		
4R-1, 34–36	219.94–219.96	117	Albian	Porcellanite		Mostly moderate orange pink (5YR 8/4) and minor pale yellowish brown (10YR 6/2)	
4R-2, 70–72	220.80–220.82	117	Albian	Chert and porcellanite	Mostly dusky brown (5YR 2/2) with moderate brown (5YR 4/4) and moderate reddish brown (10R 4/6) laminations	Minor: grayish pink (5R 8/2) and grayish orange (10YR 7/4)	
4R-1, 90–92	219.50–219.52	117	Albian	Chert and porcellanite	Dusky brown (5YR 2/2), minor moderate brown (5YR 3/4)	Minor: very pale orange (10YR 8/2)	
4R-1, 106–108	219.66–219.68	117	Albian	Chert and porcellanite	Dusky brown (5YR 2/2) and minor moderate brown (5YR 3/4)	Very pale orange (10YR 8/2)	
5R-1, 10–12	228.40–228.42	118	Albian	Chert and porcellanite	Minor: dusky brown (5YR 2/2)	Mostly grayish orange (10YR 7/4), moderate orange pink (5YR 8/4), and pale yellowish brown (10YR 6/2)	
7R-1, 59–61	247.89–247.91	119	Aptian	Chert and porcellanite	Dusky brown (5YR 2/2)		
7R-1, 97–99	248.27–248.29	119	Aptian	Porcellanite		Very pale orange (10YR 8/2)	
9R-1, 56–58	266.96–266.98	127	Hauterivian	Limestone			Very light gray (N8) to white (N9)
9R-1, 59–61	266.99–267.01	127	Hauterivian	Chert and porcellanite	Medium dark gray (N4) to medium gray (N5), minor light gray (N7)	Minor: white (N9)	
9R-1, 105–107	267.45–267.47	127	Hauterivian	Chert and porcellanite	Moderate brown (5YR 4/4) with minor grayish orange (10YR 7/4) in burrows	Yellowish gray (5Y 8/1) on edge	
9R-1, 124–127	267.64–267.67	127	Hauterivian	Chert and porcellanite	Moderate yellowish brown (10YR 6/2) with very pale orange (10YR 8/2) in burrows	Edge: white (N9)	
10R-1, 8–10	275.98–276.00	128	Hauterivian	Limestone			Yellowish gray (5Y 8/1)
10R-1, 23–25	276.13–276.15	128	Hauterivian	Porcellanite and chert	Minor flecks: dark gray (N3)	Yellowish gray (5Y 8/1) (? or limestone)	
10R-1, 49–50	276.39–276.40	128	Hauterivian	Chert and porcellanite	Medium dark gray (N4), medium gray (N5), very light gray (N8)	Very light gray (N8), minor very light gray (N8)	
11R-1, 26–28	285.46–285.48	130	Hauterivian	Chert and porcellanite	Medium gray (N5) with pinkish gray (5YR 8/1) in burrows	Edge: minor yellowish gray (5Y 8/1)	
11R-1, 35–38	285.55–285.58	130	Hauterivian	Chert and porcellanite	Medium dark gray (N4) and light gray (N7) burrow mottled	Edge: very light gray (N8)	
11R-1, 62–64	285.82–285.84	130	Hauterivian	Limestone			Light greenish gray (5GY 8/1)
14R-1, 46–48	314.56–314.58	132	Valanginian	Chert and porcellanite/chalk(?)	Medium dark gray (N4), medium gray (N5) and medium light gray (N6)	Edge: yellowish gray (5Y 8/1)	
14R-1, 49–51	314.59–314.61	132	Valanginian	Limestone			White (N9) to yellowish gray (5Y 8/1)
14R-1, 105–107	315.15–315.17	132	Valanginian	Chert and porcellanite	Medium gray (N6) and medium light gray (N6), with yellowish gray (5Y 8/1) in burrows	Edge: yellowish gray (5Y 8/1)	
15R-1, 22–24	324.02–324.04	135	Valanginian	Limestone			Yellowish gray (5Y 8/1)
15R-1, 39–43	324.19–324.23	135	Valanginian	Chert	Very light gray (N8), medium gray (N5) and medium light gray (N6), minor pale yellowish brown (10YR 6/2)		
15R-1, 71–74	324.51–324.54	135	Valanginian	Chert	Medium light gray (N6), light gray (N7) and very light gray (N8) chert, laminations, burrows		
19R-1, 19–21	362.39–362.41	137	Berriasian	Limestone			Yellowish gray (5Y 8/1), light olive-gray (5Y 6/1) and olive-gray (5Y 4/1)

Table T2 (continued).

Core, section, interval (cm)	Depth (mbsf)	Age (Ma)	Time period	Lithology	Colors		
					Chert	Porcellanite	Limestone
19R-1, 59–63	362.79–362.83	137	Berriasian	Chert	Olive-black (5Y 2/1), olive-gray (5Y 4/1), and light olive-gray (5Y 6/1)		
19R-1, 96–99	363.16–363.19	137	Berriasian	Chert and porcellanite	Brownish black (5YR 2/1)	Yellowish gray (5Y 8/1)	
19R-1, 103–105	363.23–363.25	137	Berriasian	Limestone			Yellowish gray (5Y 7/2), minor light olive-gray (5Y 5/2)
20R-1, 21–23	372.01–372.03	137	Berriasian	Limestone			Light olive-gray (5Y 5/2)
20R-1, 37–40	372.17–372.20	138	Berriasian	Limestone			Light olive-gray (5Y 5/2) and yellowish gray (5Y 7/2) laminations, partially salicified limestone(?): olive-gray (5Y 3/2) and light gray (5Y 5/2) laminations and burrow mottling
20R-1, 85–89	372.65–372.69	137	Berriasian	Chert and porcellanite/ chalk(?)	Light olive-gray (5Y 6/1) with very minor olive-gray (5Y 4/1)	Minor: yellowish gray (5Y 8/1)	
21R-1, 31–33	381.71–381.73	137	Berriasian	Limestone			Pale olive (10Y 6/2), yellowish gray (5Y 7/2), and light olive-gray (5Y 5/2) laminations
21R-1, 38–42	381.78–381.82	137	Berriasian	Chert and porcellanite	Light olive-gray (5Y 6/1), olive-gray (5Y 4/1), minor olive-black (5Y 2/1) burrow mottling	Yellowish gray (5Y 8/1)	
21R-1, 94–96	382.34–382.36	137	Berriasian	Chert	Light gray (N7) to medium light gray (N6) minor dark gray (N3), burrow mottling		
22R-1, 38–42	391.48–391.52	138	Berriasian	Limestone			Greenish gray (5GY 6/1) and yellowish gray (5Y 7/2) laminations
22R-1, 63–65	391.73–391.75	138	Berriasian	Limestone			Yellowish gray (5Y 7/2) and light olive-gray (5Y 5/2) and pale olive (10Y 6/2), slight lamination
22R-1, 120–125	392.30–392.35	138	Berriasian	Chert and limestone	Medium gray (N5) to light gray (N7), dark gray (N3) laminations		Minor: white (N9) in burrows
23R-1, 58–60	401.28–401.30	139	Berriasian	Limestone			Grayish olive (10Y 4/2) to pale olive (10Y 6/2)
23R-1, 69–71	401.39–401.41	139	Berriasian	Limestone			Grayish olive (10Y 4/2) to pale olive (10Y 6/2)
23R-1, 62–64	401.32–401.34	139	Berriasian	Limestone			Grayish olive (10Y 4/2) and pale olive (10Y 6/2)
23R-1, 66–68	401.36–401.38	139	Berriasian	Limestone			Dark greenish gray (5GY 4/1) with minor greenish gray (5GY 6/1)
23R-1, 74–76	401.44–401.46	139	Berriasian	Chert and porcellanite	Olive-gray (5Y 4/1), medium gray (N5), minor dark gray (N3) chert, yellowish gray (5Y 8/1)	Minor: dark yellowish orange (10YR 6/6)	
23R-1, 91–93	401.61–401.63	139	Berriasian	Limestone			Grayish yellow-green (5GY 7/2) to dusky yellow-green (5GY 5/2)
23R-1, 100–104	401.70–401.74	139	Berriasian	Chert and porcellanite	Olive-gray (5Y 4/1), light olive-gray (5Y6/1), olive-black (5Y 2/1), minor: greenish gray (5GY 4/1), burrow mottling	Yellowish gray (5Y 7/2)	
24R-1, 11–13	410.41–410.43	140	Berriasian	Chert and porcellanite	Light olive-gray (5Y 6/1), light gray (N7), and medium dark gray (N4), burrow mottling chert	Pinkish gray (5YR 8/1)	
24R-1, 15–17	410.45–410.47	140	Berriasian	Limestone			Light greenish gray (5GY 8/1) minor light olive-gray (5Y 6/1) and dark greenish gray (5GY 4/1)

Table T2 (continued).

Core, section, interval (cm)	Depth (mbsf)	Age (Ma)	Time period	Lithology	Colors		
					Chert	Porcellanite	Limestone
24R-1, 119–121	411.49–411.51	140	Berriasian	Chert and limestone	Moderate brown (5YR 3/4) and dark yellowish brown (10YR 4/2), minor grayish green (10GY 5/2) and dusky yellowish green (10GY 3/2)		Pale yellowish green (10GY 7/2)
25R-1, 22–26	420.12–420.16	141	Berriasian	Limestone			Pale olive (10Y 6/2), light greenish gray (5GY 8/1) and minor grayish olive (10Y 4/2)
25R-1, 42–45	420.32–420.35	141	Berriasian	Chert and limestone	Grayish green (10GY 5/2) to dusky yellow-green (5GY 5/2), minor moderate yellowish brown (10YR 5/4) and dusky yellowish green (10GY 3/2)		Pale olive (10Y 6/2)
25R-1, 49–53	420.39–420.43	141	Berriasian	Chert	Moderate yellowish brown (10YR 5/4) burrow mottled, greenish gray (5G Y6/1), and grayish green (10GY 5/2)		
25R-1, 70–76	420.60–420.66	141	Berriasian	Chert	Medium bluish gray (5B 8/1), grayish blue (5PB 5/2), and pale yellowish brown (10YR 6/2), burrow mottling(?), minor dusky yellow green (5GY 5/2) to greenish gray (10GY 5/2)		
26R-1, 18–21	429.28–429.31	142	Berriasian	Chert and porcellanite	Light olive-gray (5Y 5/2) and minor moderate yellowish brown (10YR 5/4) and dusky yellowish brown (10YR 2/2) chert	Edge: light greenish gray (5GY 8/1)	
26R-1, 53–55	429.63–429.65	142	Berriasian	Chert and porcellanite	Dark reddish brown (10R 3/4), minor very dusky red (10R 2/2)	Moderate orange-pink (5YR 8/4)	
26R-1, 66–70	429.76–429.80	142	Berriasian	Chert	Moderate yellowish brown (10YR 5/4) with minor moderate reddish orange (10YR 6/6), moderate red (5R4/6) and very pale orange (10YR 8/2)		
27R-1, 26–29	438.86–438.89	144	Berriasian	Limestone			Moderate brown (5YR 4/4)
27R-1, 40–42	439.00–439.02	144	Berriasian	Chert	Dusky yellowish brown (10YR 2/2), moderate brown (5YR 4/4), and moderate reddish orange (10R 6/6) chert, pale red (10R 6/2) chert in burrows		
27R-1, 50–53	439.10–439.30	144	Berriasian	Chert	Moderate reddish brown (10R 4/6) chert, with grayish green (10GY 5/2), pale yellowish green (10GY 7/2) fine laminations fine greenish black (5GY 2/1) in crosscutting boundary		
27R-1, 78–82	439.38–439.42	144	Berriasian	Chert	Light brown (5YR 5/6), to grayish brown (5YR 3/2), to dusky brown (5YR 2/2)		
198-1214A-							
14R-1, 20–26	120.60–120.66	107	Albian	Porcellanite		Yellowish gray (5Y 8/1) with dark gray (N3) specks	
14R-1, 53–56	120.93–120.96	107	Albian	Chert and porcellanite	Olive-gray (5Y 4/1)	Yellowish gray (5Y 8/1), minor light gray (5Y 6/1)	
14R-1, 97–100	121.37–121.40	107	Albian	Chert and porcellanite	Grayish brown (5YR 3/2)	Yellowish gray (5Y 8/1) on edge	
16R-1, 17–19	139.87–139.89	109	Albian	Chert and porcellanite	Grayish brown (5YR 3/2) to moderate brown (5YR 3/4) with light gray (N7) to white (N9) burrow mottling,	Edge: light gray (N7) to white (N9)	

Table T2 (continued).

Core, section, interval (cm)	Depth (mbsf)	Age (Ma)	Time period	Lithology	Colors		
					Chert	Porcellanite	Limestone
16R-1, 80–83	140.50–140.53	109	Albian	Chert and porcellanite	Dusky brown (5YR 2/2), pale yellowish brown (10YR 6/2)	Pinkish gray (5YR 8/1)	
198-1207B-							
40R-CC, 17–20	526.67–526.70	118	Aptian	Limestone			Yellowish gray (5Y 7/2) to light olive-gray (5Y 5/2)
40R-CC, 20–22	526.70–526.72	118	Aptian	Chert and limestone	Medium light gray (N6) to medium gray (N5)		Yellowish gray (5Y 7/2)
42R-CC, 40–42	546.20–546.22	120	Aptian	Chert and limestone	Minor: moderate brown (5YR 3/4)		Yellowish gray (5Y 7/2)
42R-CC, 44–48	546.24–546.28	120	Aptian	Chert	moderate brown (5YR 3/4) and moderate brown (5YR 4/4)		
46R-2, 7–10	585.77–585.80	122	Barremian	Chert and porcellanite	Pale yellowish brown (10YR 6/2) and dark yellowish brown (10YR 4/2), (with cross-hatching) chert, dusky yellowish brown (10YR 2/2) chert on edges		
46R-1, 134–137	585.54–585.57	122	Barremian	Chert	Medium gray (N6) chert and very light gray (N8) and dark gray (N3) in burrows		
46R-1, 141–144	585.61–585.64	122	Barremian	Chert	Light olive-gray (5Y 6/1) and olive-black (5Y 2/1)		
46R-1, 146–149	585.66–585.69	122	Barremian	Porcellanite		Yellowish gray (5Y 8/1) and light olive-gray (5Y 6/1)	
47R-2, 39–42	595.59–595.62	124	Barremian	Chert	Olive-black (5Y 2/1), light olive-gray (5Y 6/1)		
47R-2, 75–79	596.95–595.99	124	Barremian	Porcellanite		Yellowish gray (5Y 8/1) and light olive-gray (5Y 6/1)	
49R-1, 101–108	614.21–614.28	125	Barremian	Porcellanite		Olive-gray (5Y 4/1), light olive-gray (5Y 6/1), and yellowish gray (5Y 8/1)	
49R-1, 142–145	614.62–614.65	125	Barremian	Chert	Olive-black (5Y 2/1), minor light olive-gray (5Y 6/1)		

Notes: Color according to the GSA rock color chart (Rock-Color Chart Committee, 1991). Ages from Bralower et al. (2002), modified according to the revised biostratigraphic data (**Bown,** this volume).

Table T3. Petrographic observation and visual estimates of components in thin sections of selected samples. (**See table notes.** Continued on next page.)

			Matrix					Biogenic						Textures				Diagenesis		Porosity		
Core, section, interval (cm)	Hand specimen lithology	Analyses	Carbonates (%)	Fe oxides (%)	Quartz (± opal-CT) (%)	Organic matter (%)	Other	Radiolarians (%)	Radiolarian spicules (%)	Foraminifers (%)	Ostracodes (%)	Fish scales/Teeth (%)	Coccoliths (%)	Burrowed	Laminated	Cross-lamination	Other	Opal-CT lepispheres recrystallized to quartz	Carbonate filling bioclasts	Microporosity in siliceous matrix	Intraparticle porosity	Fracture porosity
198-1207B-																						
46R-2, 7–10	Chert and porcellanite		39	<1	60	1	<1 glauconite	?	?	?					X (?)	X (?)		?	?			
46R-1, 77–79	Chert	XRF, XRD	40	<1	50	0																
46R-1, 134–137	Chert		48	1	46	0		1		3	1								X			
46R-1, 141–144	Chert	XRF, XRD	2	1	94	2				3 (?)									X			
46R-1, 146–149	Porcellanite		30		63	0		7											X	X	X	X
47R-2, 39–42	Chert	XRF, XRD	2	1	92	0		2.5 (?)		2.5 (?)									X			X
47R-2, 75–79	Limestone	XRF, XRD	60	1	24	0				5				X					X	X	X	
49R-1, 101–108	Porcellanite		25	<1	70	0	<1 glauconite			2	<1	<1		X					X	X		
49R-1, 142–145	Chert		15	1	81	1				3 (?)								X	X		?	
198-1213A-																						
7R-CC, 0–3	Chert and porcellanite	XRF, XRD	3	1	96	0				?							Cracks (?)			X		X
8R-CC, 9–12	Chert and porcellanite		15	3	75	?				6 (?)	1						Cracks (?)		X		X	
8R-CC, 12–15	Porcellanite and chert		2		90	0			?	7 (?)	<1		<1						X	X	X	
12R-1, 22–27	Porcellanite		12		78	0		4	2	5	<1		<1						X	X	X	X
12R-1, 22–27	Porcellanite	XRF, XRD	25	<1	65	0		9	2										X	X	X	X
12R-1, 36–40	Chert and limestone		25		70	0		5											X	X	X	
15R-1, 64–67	Porcellanite and chert		3		93	0				4	<1		<1						X	X		
15R-1, 77–80	Chert and porcellanite		3		85	0		3	1	8			<1						X	X	X	X
16R-1, 101–104	Chert and porcellanite		3		89	0		3	<1	4									X	X		
20R-1, 5–10	Chert and porcellanite		10		85	0		5											X		X	
21R-1, 36–40	Chert and porcellanite	XRF, XRD	2		83	?		10		5								X	X	X		X
198-1213B-																						
1R-1, 28–30	Chert		3	1	85	0		1		9	<1	<<1	3					X	X		X	X
1R-1, 52–54	Chert		1	<1	78	?		1		18							Cracks	X	X			
1R-1, 57–59	Chert	XRF, XRD	5	<1	85	1		3	1	6	<1							X	X	X	X	
3R-1, 41–43	Chert and porcellanite	XRF, XRD	3	2	92	?		tr(?)		3	<1							X	X	X	X	X
3R-1, 53–55	Chert and porcellanite		3		94	?	<1 barite	tr(?)		3							Major veins	X		X	X	X
3R-1, 73–75	Chert and porcellanite	XRF, XRD	3	<1	70	?	<1 glauconite	7	2	10	<1							X	X	X	X	
4R-1, 34–36	Quartz veins	XRF, XRD	8		80	0		11	1								Major quartz-filled veins		X	X	X	
4R-1, 90–92	Chert and porcellanite		30	<1	54	1		<1		15								X	X	X	X	X
4R-1, 106–108	Chert and porcellanite	XRF, XRD	2	<1	85	1		3	3	5	<1							X	X	X		X
7R-1, 59–61	Chert and porcellanite	XRF, XRD	4	<1	87	0		3	<1	4	<1		<1					X	X	X	X	X
7R-1, 97–99	Porcellanite	XRF, XRD	15	<1	65	0		19	1	<1	<1								X			
9R-1, 59–61	Chert and porcellanite	XRF, XRD	4		90	0		6											X		X	X

Table T3 (continued).

Core, section, interval (cm)	Hand specimen lithology	Analyses	Matrix					Biogenic						Textures				Diagenesis		Porosity		
			Carbonates (%)	Fe oxides (%)	Quartz (± opal-CT) (%)	Organic matter (%)	Other	Radiolarians (%)	Radiolarian spicules (%)	Foraminifers (%)	Ostracodes (%)	Fish scales/Teeth (%)	Coccoliths (%)	Burrowed	Laminated	Cross-lamination	Other	Opal-CT lepispheres recrystallized to quartz	Carbonate filling bioclasts	Microporosity in siliceous matrix	Intraparticle porosity	Fracture porosity
9R-1, 124–127	Chert and porcellanite	XRF, XRD	3	<1	90	0	1 opaque	5					<1						X			X
10R-1, 8–10	Limestone	XRF, XRD	75	<1	20	0	2 opaques	5					<1							X	X	
19R-1, 19–21	Limestone		92	2		0	5 opaques			<1	<1	<<1							X		X	X
19R-1, 59–63	Chert	XRF, XRD	4	<1	91	1				3								X	X		X	
19R-1, 96–99	Chert and porcellanite	XRF, XRD	1	<1	89	?		8	<1	2									X			X
19R-1, 103–105	Limestone	XRF, XRD	86	1	6	0	<1 glauconite	4	<1	<1		<1		X (?)						X	X	
20R-1, 21–23	Limestone		93	1		0	5 opaques			<1									X	X	X	X
20R-1, 37–40	Limestone		82	1	7	0	<1 glauconite	5	2	3		<1							X	X	X	X
20R-1, 85–89	Chert and porcellanite/chalk		5	3	84	0	3 opaque	4	1	1									X		X	
21R-1, 31–33	Limestone	XRF	70		26	0	2 opaques	2											X	X	X	
22R-1, 38–42	Limestone		95	1		0	3 opaque	2		3					X				?	X		X
22R-1, 63–65	Limestone		85	<1		0	1 opaque	8	2	5									X	X	X	
22R-1, 120–125	Chert and limestone	XRF, XRD	5	<1	98	0	4 opaques	1		4	<1	<1						X	X		X	
23R-1, 58–60	Limestone		90	<1	2	0		8	1					X (?)	X					X	X	X
23R-1, 62–64	Limestone		89	<1	3	0		7	1						X					X	X	X
23R-1, 66–68	Limestone		93	<1	3	0		7							X					X		X
23R-1, 74–76	Chert and porcellanite		3	2	95	1	<1 glauconite	0.5 (?)		0.5 (?)									X		X	X
25R-1, 22–26	Limestone	XRF, XRD	92	<1	3	0		5 (?)											X	X	X	X
25R-1, 70–76	Chert	XRF, XRD	10	<1	86	0		3											X			
26R-1, 18–21	Chert and porcellanite		4	1	82	0		20	1									X	X	X		
26R-1, 53–55	Chert and porcellanite	XRF, XRD	10	<1	82	1	<1 glauconite	5										X	X			X
26R-1, 66–70	Chert	XRF, XRD	1	<1	84	2		15		?		<1		X				X	X			
27R-1, 26–29	Limestone		80	<1	5	0		15										X		X	X	
27R-1, 40–42	Chert		5	1	85	1		8	1	?			<1	X (?)				X	X	X		
27R-1, 50–53	Chert		5	<1	95	0		4											X			
27R-1, 78–82	Chert	XRF, XRD	2	<1	88	1		15		5 (?)												
198-1214A-																						
14R-1, 20–26	Chert		73		15	0		2	1	9								X	X	X		X
14R-1, 53–56	Chert and porcellanite		5		85	0		1		9								X	X		X	
14R-1, 97–100	Chert and porcellanite		2	1	87	?		9			1								X	X		X
16R-1, 17–19	Chert and porcellanite		3	1	80	0		13	1	1	<1							X	X	X	X	
16R-1, 80–83	Chert and porcellanite		2	<1	83	0		6	1	7									X		X	X

Notes: XRF = X-ray fluorescence, XRD = X-ray diffraction. X = present.

Table T4. XRF data for chert, porcellanite, and limestone samples, Sites 1207 and 1213. (See table notes. Continued on next three pages.)

Hole:		198-1207B-				198-1213A-			198-1213B-						
Core, section, interval (cm):		46R-1, 77–79	46R-1, 141–144	47R-2, 39–42	47R-2, 75–79	7R-CC, 0–3	12R-1, 22–27	21R-1, 36–40	1R-1, 57–59	3R-1, 41–43	3R-1, 73–75	4R-1, 34–36	4R-1, 106–108	7R-1, 59–61	7R-1, 97–99
Rock type:		Calcareous pale orange chert	Brown chert	Gray chert	Limestone	Brown chert	Calcareous porcellanite	Red chert	Red chert	Red chert	Brown chert	Porcellanitic pale orange chert	Brown chert	Red chert	Porcellanitic pale orange chert
Limit of detection:															
SO_3		0.90	0.03	0.03	0.37		0.12					0.00			0.11
Cl		0.43	0.00	0.01	0.46		0.14					0.03			0.08
Unnormalized major elements (wt%):															
SiO_2	0.1	53.97	97.27	89.72	24.40	95.67	68.53	97.27	97.37	97.06	97.07	83.70	96.25	96.36	73.37
TiO_2	0.005	0.17	0.02	0.02	0.13	0.01	0.05	0.01	0.01	0.02	0.03	0.10	0.04	0.03	0.09
$Al2O_3$	0.05	2.80	0.19	0.18	2.28	0.37	0.70	0.37	0.38	0.52	0.57	1.60	0.71	0.64	1.33
FeO	0.03	1.03	–0.11	–0.15	0.57	0.15	–0.01	0.12	0.20	0.27	0.21	0.64	0.32	0.32	0.48
MnO	0.001	0.01	0.00	0.00	0.02	0.04	0.01	0.00	0.00	0.00	0.00	0.03	0.07	0.01	0.02
MgO	0.03	0.72	–0.05	0.01	0.70	0.13	0.21	0.09	0.00	0.08	0.09	0.45	0.13	0.15	0.35
CaO	0.02	34.02	0.78	8.45	58.14	0.85	26.80	0.25	0.23	0.11	0.17	10.05	0.12	0.19	21.25
Na_2O	0.03	0.64	0.06	0.04	0.40	0.20	0.24	0.14	0.10	0.16	0.20	0.50	0.16	0.24	0.45
K_2O	0.02	0.65	0.09	0.09	0.33	0.12	0.30	0.11	0.11	0.16	0.19	0.50	0.23	0.22	0.33
P_2O_5	0.002	0.12	0.03	0.03	0.19	0.49	0.10	0.02	0.03	0.03	0.02	0.11	0.03	0.03	0.05
Total:		94.13	98.27	98.39	87.18	98.02	96.94	98.39	98.44	98.42	98.54	97.69	98.06	98.19	97.71
LOI (wt%):		23.64	1.63	6.83	33.69		19.37					9.84			16.31
Total with SO_3, Cl:		95.46	98.30	98.44	88.00		97.20					97.72			97.89
Normalized major elements (wt%):															
SiO_2		57.34	98.98	91.19	27.99	97.60	70.69	98.87	98.92	98.62	98.51	85.69	98.16	98.14	75.09
TiO_2		0.180	0.016	0.016	0.150	0.012	0.049	0.013	0.014	0.024	0.026	0.099	0.038	0.031	0.089
Al_2O_3		2.97	0.19	0.18	2.62	0.38	0.73	0.38	0.39	0.53	0.58	1.64	0.72	0.65	1.36
FeO*		1.10	0.00	0.00	0.66	0.15	0.00	0.13	0.20	0.28	0.21	0.66	0.33	0.33	0.49
MnO		0.011	0.002	0.003	0.026	0.036	0.014	0.000	0.001	0.002	0.002	0.032	0.067	0.010	0.020
MgO		0.77	0.00	0.01	0.80	0.13	0.22	0.09	0.00	0.08	0.09	0.46	0.13	0.15	0.35
CaO		36.14	0.79	8.59	66.70	0.87	27.65	0.25	0.23	0.11	0.17	10.29	0.12	0.19	21.75
Na_2O		0.69	0.09	0.09	0.38	0.20	0.31	0.14	0.10	0.16	0.20	0.51	0.16	0.24	0.34
K_2O		0.68	0.06	0.04	0.46	0.12	0.25	0.11	0.11	0.16	0.19	0.51	0.23	0.22	0.46
P_2O_5		0.126	0.027	0.027	0.220	0.495	0.098	0.019	0.035	0.031	0.018	0.117	0.035	0.025	0.050
Total:		100.00	100.00	100.00	100.00	100.00	100.00	100.00	100.00	100.00	100.00	100.00	100.00	100.00	100.00
Unnormalized trace elements (ppm):															
Ni	1.4	15	12	8	9	18	3	9	7	10	15	18	10	11	9
Cr	1.0	34	9	6	24	0	6	0	0	0	0	11	0	0	7
Sc	1.2	11	2	2	7	4	7	1	1	3	0	5	0	6	6
V	3.0	66	7	7	45	1	10	5	0	0	0	11	0	0	10
Ba	7.9	4825	32	55	4507	14	938	0	6	5	5	1549	90	9	954
Rb	1.1	22	3	3	17	3	9	4	2	6	6	20	7	7	16
Sr	0.9	764	11	57	859	38	421	6	7	7	7	139	9	6	190
Zr	1.3	54	13	14	57	10	27	7	7	8	9	31	10	9	31
Y	1.2	33	7	8	44	98	26	7	11	10	7	22	9	6	17
Nb	0.5	5.2	1.7	2.9	4.3	1.6	2.6	1.2	0.2	1.7	0.8	3.5	1.8	3.1	3.8
Ga	2.4	6	0	1	2	3	3	0	1	0	2	2	0	3	3
Cu	1.4	45	12	11	17	13	15	7	4	9	7	32	12	11	20
Zn	2.2	33	15	8	74	11	15	5	3	8	3	27	16	5	20

Table T4 (continued).

Hole:		198-1213B-													
Core, section, interval (cm):		9R-1, 59–61	9R-1, 124–127	10R-1, 8–10	19R-1, 59–63	19R-1, 96–99	19R-1, 103–105	21R-1, 31–33	22R-1, 120–125	25R-1, 22–26	25R-1, 70–76	25R-1, 70–76	26R-1, 53–55	26R-1, 66–70	27R-1, 78–82
Rock type:		Dark gray chert	Brown chert	Limestone	Gray chert	Gray chert	Siliceous limestone	Siliceous limestone	Gray chert	Limestone	Green chert	Gray chert	Brown chert	Brown chert	Brown chert
Limit of detection:															
SO_3		0.01	0.00	0.19			0.66	0.53		0.17	0.05	0.03			
Cl		0.00	0.00	0.93			0.45	0.55		0.45	0.00	0.00			
Unnormalized major elements (wt%):															
SiO_2	0.1	97.35	97.73	17.67	96.29	95.60	33.25	24.61	95.34	3.50	94.92	96.81	69.78	95.55	93.39
TiO_2	0.005	0.03	0.03	0.15	0.01	0.01	0.12	0.14	0.01	0.05	0.01	0.01	0.03	0.01	0.02
$Al2O_3$	0.05	0.44	0.44	2.53	0.30	0.36	2.15	2.36	0.30	0.80	0.26	0.15	0.52	0.23	0.47
FeO	0.03	–0.06	0.08	0.70	0.20	1.14	3.15	2.74	0.17	1.29	0.05	–0.09	0.00	0.39	1.74
MnO	0.001	0.00	0.00	0.08	0.00	0.00	0.08	0.12	0.01	1.29	0.07	0.01	0.89	0.08	0.79
MgO	0.03	–0.03	–0.04	0.78	0.07	0.09	1.71	1.10	0.05	0.81	0.00	0.00	0.27	0.06	0.21
CaO	0.02	0.08	0.03	63.40	1.04	0.16	47.24	55.29	1.93	71.77	2.44	0.70	18.52	1.47	0.20
Na_2O	0.03	0.15	0.16	0.63	0.19	0.20	0.62	0.46	0.10	0.17	0.17	0.20	0.12	0.16	0.18
K_2O	0.02	0.16	0.15	0.56	0.07	0.09	0.52	0.70	0.08	0.27	0.13	0.05	0.28	0.06	0.20
P_2O_5	0.002	0.04	0.02	0.06	0.03	0.03	0.32	0.19	0.04	0.19	0.04	0.05	0.06	0.04	0.09
Total:		98.15	98.61	86.57	98.20	97.67	89.16	87.71	98.02	80.13	98.08	97.82	90.47	98.05	97.29
LOI (wt%):		1.53	1.70	38.84			29.60	33.55		40.43	2.32	1.42			
Total with SO_3, Cl:		98.17	98.61	87.69			90.27	88.79		80.75	98.13	97.85			
Normalized major elements (wt%):															
SiO_2		99.18	99.11	20.41	98.05	97.88	37.29	28.05	97.26	4.36	96.78	98.97	77.13	97.45	95.99
TiO_2		0.031	0.031	0.170	0.009	0.009	0.131	0.165	0.007	0.060	0.014	0.013	0.029	0.006	0.024
Al_2O_3		0.45	0.44	2.93	0.31	0.37	2.42	2.69	0.31	1.00	0.26	0.15	0.57	0.23	0.48
FeO*		0.00	0.08	0.81	0.21	1.16	3.53	3.12	0.17	1.60	0.05	0.00	0.00	0.40	1.79
MnO		0.000	0.000	0.094	0.001	0.000	0.093	0.137	0.006	1.605	0.073	0.014	0.986	0.084	0.808
MgO		0.00	0.00	0.91	0.07	0.09	1.92	1.25	0.05	1.01	0.00	0.00	0.30	0.06	0.22
CaO		0.08	0.04	73.24	1.06	0.16	52.98	63.04	1.97	89.56	2.49	0.71	20.47	1.50	0.21
Na_2O		0.16	0.16	0.64	0.19	0.20	0.58	0.52	0.10	0.21	0.17	0.20	0.13	0.16	0.19
K_2O		0.16	0.17	0.72	0.07	0.09	0.69	0.80	0.08	0.34	0.13	0.06	0.31	0.06	0.21
P_2O_5		0.038	0.021	0.074	0.029	0.030	0.364	0.219	0.039	0.241	0.045	0.049	0.063	0.041	0.096
Total:		100.00	100.00	100.00	100.00	100.00	100.00	100.00	100.00	99.99	100.01	100.17	100.00	100.00	100.00
Unnormalized trace elements (ppm):															
Ni	1.4	20	11	0	18	41	27	31	23	20	38	17	5	9	14
Cr	1.0	9	7	12	3	13	32	33	0	11	11	12	0	1	26
Sc	1.2	1	1	6	3	6	9	8	6	0	1	2	0	2	1
V	3.0	6	4	31	3	13	70	68	6	53	11	8	75	0	10
Ba	7.9	15	15	3104	504	0	12361	5390	431	10722	124	22	2947	92	40
Rb	1.1	5	6	21	5	1	19	20	3	9	8	3	9	2	6
Sr	0.9	4	3	1026	39	8	775	712	33	767	23	9	129	14	13
Zr	1.3	16	16	56	7	8	58	62	8	44	15	14	14	8	13
Y	1.2	8	5	34	6	7	72	45	10	57	9	8	23	10	15
Nb	0.5	3.8	3.5	4.7	1.2	0.9	3.4	4.2	1.7	2.0	2.8	2.7	1.3	2.7	2.3
Ga	2.4	2	0	2	3	2	3	4	1	1	0	2	3	2	3
Cu	1.4	13	6	0	19	24	106	93	32	16	14	11	26	14	50
Zn	2.2	14	4	44	8	36	60	90	14	82	6	21	17	3	11

Table T4 (continued).

Hole:		198-1207B-				198-1213A-			198-1213B-						
Core, section, interval (cm):		46R-1, 77–79	46R-1, 141–144	47R-2, 39–42	47R-2, 75–79	7R-CC, 0–3	12R-1, 22–27	21R-1, 36–40	1R-1, 57–59	3R-1, 41–43	3R-1, 73–75	4R-1, 34–36	4R-1, 106–108	7R-1, 59–61	7R-1, 97–99
Rock type:		Calcareous pale orange chert	Brown chert	Gray chert	Limestone	Brown chert	Calcareous porcellanite	Red chert	Red chert	Red chert	Brown chert	Porcellanitic pale orange chert	Brown chert	Red chert	Porcellanitic pale orange chert
Limit of detection:															
Unnormalized trace elements (ppm):															
Pb	2.0	7	3	3	1	0	4	0	0	0	0	4	0	0	4
La	3.6	29	3	3	23	71	17	4	11	15	13	9	23	5	17
Ce	5.0	7	6	8	3	12	10	4	0	16	4	15	10	10	13
Th	1.9	5	1	2	1	1	1	0	0	0	0	4	2	1	2
Total trace elements (ppm):		5961	137	197	5695	393	1516	60	60	20052	666	1903	2260	92	1321
Total trace elements (%):		0.60	0.01	0.02	0.57	0.04	0.15	0.06	0.0602	2.01	0.07	0.19	0.23	0.0921	0.13
Total major and trace elements (%):		96.06	98.31	98.45	88.57	100.00	97.36	100.00	100	100.00	100.00	97.91	100.00	100.00	100.00

Notes: Major elements are normalized on a volatile-free basis. * = Fe expressed as FeO.

Table T4 (continued).

Hole:		198-1213B-													
Core, section, interval (cm):		9R-1, 59–61	9R-1, 124–127	10R-1, 8–10	19R-1, 59–63	19R-1, 96–99	19R-1, 103–105	21R-1, 31–33	22R-1, 120–125	25R-1, 22–26	25R-1, 70–76	25R-1, 70–76	26R-1, 53–55	26R-1, 66–70	27R-1, 78–82
Rock type:		Dark gray chert	Brown chert	Limestone	Gray chert	Gray chert	Siliceous limestone	Siliceous limestone	Gray chert	Limestone	Green chert	Gray chert	Brown chert	Brown chert	Brown chert
Limit of detection:															
Unnormalized trace elements (ppm):															
Pb	2.0	3	4	9	0	0	1	9	0	2	3	5	1	0	5
La	3.6	1	5	30	12	10	40	26	26	34	5	4	28	19	16
Ce	5.0	2	6	18	9	5	0	0	3	0	7	6	0	0	0
Th	1.9	2	1	1	2	0	2	5	0	3	1	1	0	0	0
Total trace elements (ppm):		126	100	4400	3256	260	13640	6599	101	11823	279	149	17702	15745	4227
Total trace elements (%):		0.01	0.01	0.44	0.33	0.03	1.36	0.66	0.01	1.18	0.03	0.01	1.77	1.57	0.42
Total major and trace elements (%):		98.18	98.62	88.13	100.00	100.00	91.63	89.45	100.00	81.93	98.16	97.87	100.00	100.00	100.00

Table T5. Correlation coefficient matrix relating major and minor element compositions.

	SiO_2	TiO_2	Al_2O_3	FeO*	MnO	MgO	CaO	Na_2O	K_2O	P_2O_5	Ni	Cr	Sc
SiO_2	1.00000												
TiO_2	–0.80117	1.00000											
Al_2O_3	–0.80112	0.99323	1.00000										
FeO*	–0.62848	0.59130	0.61916	1.00000									
MnO	–0.43223	–0.00656	–0.00930	0.26748	1.00000								
MgO	–0.86375	0.80773	0.83015	0.86212	0.26799	1.00000							
CaO	–0.99869	0.78191	0.78008	0.59367	0.43942	0.84019	1.00000						
Na_2O	–0.67493	0.92964	0.93303	0.59777	–0.09900	0.77608	0.64861	1.00000					
K_2O	–0.79125	0.95850	0.95778	0.69018	0.10556	0.86386	0.76595	0.92318	1.00000				
P_2O_5	–0.510685	0.39619	0.42686	0.53783	0.21839	0.62738	0.49481	0.40697	0.43551	1.00000			
Ni	–0.003427	–0.02854	–0.00949	0.43425	–0.01406	0.18342	–0.01530	0.06135	0.03071	0.21907	1.00000		
Cr	–0.59198	0.73462	0.72412	0.78227	0.09907	0.72493	0.56257	0.70389	0.69983	0.40553	0.37091	1.00000	
Sc	–0.47583	0.71437	0.72668	0.49034	–0.31916	0.58865	0.45410	0.78108	0.66578	0.38123	0.17230	0.58834	1.00000
V	–0.77644	0.70121	0.70702	0.65195	0.45887	0.81104	0.76073	0.60592	0.74960	0.46217	0.15983	0.67774	0.44531
Ba	–0.84812	0.63155	0.64959	0.76312	0.48335	0.92661	0.83445	0.57823	0.68632	0.60726	0.20386	0.61313	0.40377
Rb	–0.73004	0.95416	0.94255	0.55256	0.30285	0.77900	0.70798	0.92733	0.96322	0.36178	–0.01816	0.67100	0.66231
Sr	–0.95845	0.88850	0.89315	0.59944	0.23819	0.86220	0.95284	0.80068	0.84093	0.49628	–0.03805	0.66103	0.62085
Zr	–0.91612	0.94881	0.93745	0.67585	0.15523	0.89338	0.90241	0.85932	0.91472	0.50849	0.06272	0.77959	0.66178
Nb	–0.52204	0.77658	0.73086	0.31637	–0.14243	0.49787	0.51035	0.73484	0.69371	0.18962	–0.04939	0.62862	0.59747
Ga	–0.35744	0.52772	0.53487	0.43741	0.09614	0.46745	0.33279	0.62552	0.54378	0.41641	0.03855	0.53591	0.64766
Cu	–0.41535	0.50216	0.52124	0.88822	0.11010	0.74507	0.37567	0.53396	0.61206	0.49220	0.47060	0.75624	0.53971
Zn	–0.89777	0.72682	0.72950	0.73643	0.36238	0.83548	0.88949	0.59157	0.71750	0.58949	0.30007	0.68946	0.48142
Pb	–0.48288	0.66305	0.60060	0.34817	0.04065	0.39718	0.47252	0.65061	0.64330	0.05425	0.00234	0.63206	0.38771
La	–0.44729	0.33224	0.37816	0.37598	0.26966	0.50045	0.43595	0.35156	0.38999	0.85587	0.04047	0.18134	0.32895
Ce	0.09710	0.13451	0.11857	–0.33940	–0.39407	–0.16395	–0.09203	0.25317	0.10308	–0.08856	–0.27074	–0.26394	0.20887
Th	–0.52101	0.67581	0.63145	0.47848	0.05163	0.56816	0.50323	0.66267	0.67128	0.36229	0.24211	0.59983	0.49937

Note: * = Fe expressed as FeO.

Table T5 (continued).

	V	Ba	Rb	Sr	Zr	Nb	Ga	Cu	Zn	Pb	La	Ce	Th
SiO_2													
TiO_2													
Al_2O_3													
FeO*													
MnO													
MgO													
CaO													
Na_2O													
K_2O													
P_2O_5													
Ni													
Cr													
Sc													
V	1.00000												
Ba	0.82519	1.00000											
Rb	0.67852	0.60687	1.00000										
Sr	0.75946	0.79524	0.80128	1.00000									
Zr	0.77667	0.78707	0.89273	0.95363	1.00000								
Nb	0.41590	0.34067	0.75911	0.61963	0.73793	1.00000							
Ga	0.53470	0.37691	0.51881	0.44317	0.47761	0.40429	1.00000						
Cu	0.65221	0.63613	0.51804	0.42453	0.55859	0.30796	0.52489	1.00000					
Zn	0.75478	0.80995	0.63432	0.82869	0.85329	0.43775	0.33073	0.56127	1.00000				
Pb	0.40363	0.22777	0.65125	0.54344	0.64263	0.72996	0.31989	0.30649	0.41187	1.00000			
La	0.42679	0.48281	0.29144	0.45156	0.37820	0.06465	0.41431	0.33403	0.38354	–0.00398	1.00000		
Ce	–0.34904	–0.31126	0.21959	–0.00449	–0.01608	0.22325	–0.09517	–0.38411	–0.23256	0.18757	0.02227	1.00000	
Th	0.51298	0.51961	0.70107	0.53610	0.67436	0.61731	0.47706	0.50132	0.57762	0.55477	0.18522	0.09548	1.00000

Table T6. Summary of XRD data showing relative importance of components based on peak heights. Hand specimen lithology and revised lithology based on XRD data are also given.

Core, section, interval (cm)	Field description (hand specimen)	XRD results			Classification (based on XRD and field description)
		Quartz	Opal-CT	Carbonate	
198-1207B-					
46R-1, 77–79	Limestone	A	M	A	Calcareous chert
46R-1, 141–144	Chert	A	M	—	Chert
47R-2, 39–42	Chert	A	M	—	Chert
47R-2, 75–79	Limestone	M	M	A	Limestone
198-1213A-					
7R-CC, 0–3	Chert	A	M	—	Chert
12R-1, 22–27	Porcellanite	M	A	A	Calcareous porcellanite
21R-1, 36–40	Chert	A	M	—	Chert
198-1213B-					
1R-1, 57–59 (1)	Chert	A	M	—	Chert
1R-1, 57–59 (2)	Chert	A	M	—	Chert
3R-1, 41–43	Chert	A	M	—	Chert
3R-1, 73–75	Chert	A	M	—	Chert
4R-1, 34–36	Porcellanite	A	C	M	Porcellanitic chert
4R-1, 106–108	Chert	A	M	—	Chert
7R-1, 59–61	Chert	A	M	—	Chert
7R-1, 97–99	Porcellanite	A	C	C	Porcellanitic chert
9R-1, 59–61	Chert	A	M	—	Chert
9R-1, 124–127	Chert	A	M	—	Chert
10R-1, 8–10	Limestone	—	—	A	Limestone
19R-1, 59–63	Chert	A	—	—	Chert
19R-1, 96–99	Chert	A	M	—	Chert
19R-1, 103–105	Limestone	A	M	A	Siliceous limestone
22R-1, 120–125	Chert	A	M	—	Chert
25R-1, 22–26	Limestone	—	—	A	Limestone
25R-1, 70–76 (1)	Chert	A	M	—	Chert
25R-1, 70–76 (2)	Chert	A	M	—	Chert
26R-1, 53–55	Chert	A	M	—	Chert
26R-1, 66–70	Chert	A	M	—	Chert
27R-1, 78–82	Chert	A	M	—	Chert

Notes: XRD = X-ray diffraction. A = abundant, C = common, M = minor. — = not present.